Clin Neuroradiol (2019) 29:191–213
https://doi.org/10.1007/s00062-019-00773-5

REVIEW ARTICLE

Incidentalomas in Spine and Spinal Cord Imaging

Shivaprakash B. Hiremath[1] · José Boto[1] · Alice Regnaud[1] · Léonard Etienne[1] · Aikaterini Fitsiori[1] · Maria Isabel Vargas[1]

Received: 15 January 2019 / Accepted: 27 February 2019 / Published online: 18 March 2019

Abstract
Incidentalomas are common in magnetic resonance imaging (MRI) of the spine. These incidental findings (IFs) can be seen involving the spinal cord, nerve root, vertebral body, posterior arch and the extraspinal region. This review article describes the imaging findings, stratifies the IFs similar to the computed tomography (CT) colonography reporting and data system and briefly mentions the current recommendations for further evaluation and management of IFs. Radiologists are the first to detect these lesions, suggest further evaluation and management of IFs. It is therefore mandatory for them to be aware of recommendations in clinical practice in order to avoid increased patient anxiety, excessive healthcare expenditure and inadvertent therapeutic procedures.

Keywords Incidentalomas · Spine and spinal cord · MRI · CT · Syrinx

Introduction

Incidentalomas are findings discovered on imaging when examining for an unrelated clinical symptom or suspicion [1]. The widespread availability of picture archiving and communication systems (PACS), improved soft tissue resolution of magnetic resonance imaging (MRI) and the risk related to medicolegal implications lead to an increase in the number of reported incidental findings (IFs) and follow-up examinations [2].

The prevalence of IFs on spinal imaging shows an increasing trend with age due to the senile changes involving the extraspinal region in a clinically asymptomatic patient. The reported prevalence rates are variable, ranging from 8% in cervical, 4.7% in thoracic and 9.4% in the lumbar spine in the pediatric population to 25.7–29.1% in cervical, 10.5–32.2% in thoracic and 14.2–68.6% in the lumbar spine in the adult population [3–7]. The risks associated with reporting IFs include increased anxiety, healthcare expenditure and inadvertent invasive procedures for the patient along with increased workload and distraction from the primary issue of concern to radiologists.

In this review, IFs are classified based on their location into those involving the spinal cord and nerve roots, i. e., intramedullary, intradural extramedullary and neural foraminal lesions, the spine, i. e., vertebral body and arch, disc and ligaments, and extraspinal findings as depicted in Table 1, 2 and 3. The IFs are also stratified based on the need for further imaging, follow-up and need for intervention into the E1 category (normal examination or anatomical variant) when no spinal or extraspinal abnormalities are seen, E2 category (clinically unimportant finding) in cases with findings which require no further evaluation, E3 category (likely unimportant, incompletely characterized) which is likely benign and may need further work-up depending on the clinical scenario and E4 category (potentially important finding) which needs further work-up based on accepted practice guidelines and communication to the referring physician according to the CT colonography reporting and data system (C-RADS) [8]. It is better to include the description than just the numerical category in the actual report to avoid confusion regarding further evaluation. This article focuses on IFs based on their location and risk stratification as the awareness of IFs and adequate knowledge regarding the need for further imaging, follow-up, and intervention is mandatory to avoid the untoward risks involved with identification and reporting of IFs.

✉ Maria Isabel Vargas
maria.i.vargas@hcuge.ch

[1] Division of Diagnostic and Interventional Neuroradiology, Geneva University Hospitals, Rue Gabrielle-Perret-Gentil 4, 1211 Genève 14, Switzerland

Table 1 Tips and recommendations for incidentalomas of the spinal cord and nerve roots

Spinal cord and nerve roots	Imaging and clinical evaluation	Category
Syringohydromyelia	Location, length and diameter Look for underlying etiology	E2—Idiopathic syrinx E4—Syrinx with underlying etiology
Ventriculus terminalis	Look for associated altered cord signal intensity and internal septations	E2—Asymptomatic VT E3—Suspected malignant etiology—needs contrast study E4—Symptomatic VT
Lipoma of the filum terminale	Look for associated abnormalities	E2—Asymptomatic LFT E4—Symptomatic LFT with tethered cord VT with associated scoliosis
CSF flow artifacts	Change the phase and frequency encoding direction Increase the number of excitations, Assess sequences like gradient recalled echo in axial plane	E1—Normal study
Enhancement of radicular vein and vein of the filum terminale	Avoid misdiagnosis as nerve root enhancement (polyneuroradiculitis)	E1—Normal study
Perineural cysts	Location, size and bony erosion Ancillary findings—Epidural fluid and signs of intracranial hypotension in meningeal root cysts	E2—Asymptomatic cysts E3—Associated intracranial hypotension—needs myelography for further evaluation E4—Symptomatic cysts

E1 category—normal examination or anatomical variant, E2 category—clinically unimportant finding, E3 category—likely unimportant, incompletely characterized, and E4 category—potentially important finding
CSF cerebrospinal fluid, *LFT* lipoma of the filum terminale, *VT* ventriculus terminalis

Incidentalomas in Spinal Cord and Nerve Roots

The IFs involving the spinal cord, nerve roots and the spinal canal are intramedullary lesions involving the spinal cord, intradural extramedullary when located in the spinal canal and extradural lesions when they occur along the spinal nerve roots.

Syringohydromyelia

Syringomyelia is a cavity in the spinal cord due to cerebrospinal fluid (CSF) dissecting the adjacent white matter, which explains the lack of the ependymal lining, in contrast to hydromyelia, which consists of dilatation of the central canal lined by ependyma. Since these entities cannot be differentiated on imaging or pathology, the term syringohydromyelia is used. The syrinx needs careful evaluation for associated abnormalities including Chiari malformation, scoliosis, and craniovertebral junction abnormalities; however, it can also be idiopathic and secondary to neoplasms, trauma, arachnoiditis, and spondylitis (Figs. 1 and 2; [9]).

The salient features to be described in the evaluation of syringomyelia include size, craniocaudal extent, level of cord involvement, position within the cross-section of the spinal cord (central or eccentric) and altered signal intensity involving the adjacent spinal cord. A thin and linear cystic cavity in the absence of any etiology predisposing to syringomyelia, located in the region of the central canal. i.e. junction of the ventral one third and dorsal two thirds of the spinal cord and not eccentrically located, is called a persistent or prominent central canal [10, 11]. The location and diameter of the syrinx usually depends on the underlying etiology. Syrinx associated with Chiari malformation usually involves the cervical cord; tethered cord and spinal dysraphism involve the dorsal cord and idiopathic syringomyelia predominantly the cervicothoracic region [12, 13]. In a study by Strahle et al. the diameter of the syrinx increased in the following order: idiopathic < tethered cord and spinal dysraphism < Chiari malformation [12]. The syrinx shows short or long segment hypodensity on CT with signal intensity following that of cerebrospinal fluid (CSF) on T1 and T2 weighted MRI. A larger diameter, intralesional nodularity, altered signal intensity and mass adjacent to the syrinx on T2 weighted imaging suggest a neoplastic etiology [14, 15]. Initial imaging of the syrinx needs gadolinium administration to rule out an underlying occult malignancy. Idiopathic syrinx is likely in the absence of underlying associated etiology or mass lesion. In cases of idiopathic syrinx, the presence of flow voids on pre-operative T2 weighted imaging may indicate likely response post-syrinx subarachnoid shunting [15]. Asymptomatic syrinx is usually followed up annually with MRI to look for progression or more frequently if it becomes symptomatic [16]. The stability of the syrinx as demonstrated by follow-up imaging for more than 12 months in an asymptomatic patient could probably suffice to stop surveillance [11]. Usually, asymptomatic patients with a localized syrinx

Table 2 Tips and recommendations for incidentalomas in vertebral body and posterior arch

Vertebral body and posterior arch	Imaging and clinical evaluation	Category
Incomplete vertebral fusion/cleft of C1	Look for corticated margins Avoid misdiagnosis with fractures and metastasis	E1—Anatomical variant E4—Severe abnormalities associated with myelopathy or cervical instability (rare)
Block vertebra	Look for associated abnormalities and syndromic association	E2—Isolated block vertebra E4—Associated with abnormalities
Butterfly vertebra	Look for sclerotic border and midsagittal constriction Avoid misdiagnosis with fractures	E1—Anatomical variant E4—When associated with scoliosis
Vertebral hemangioma	Location and extraspinal/epidural/neural foraminal component Polka dot sign/corduroy sign on CT	E2—Typical vertebral hemangioma E4—Atypical and aggressive hemangioma E4—Advanced imaging to rule out metastasis (rare)
Bone island/enostosis	Location and brush border appearance	E2—Clinically unimportant finding, no further evaluation
Benign notochord cell tumor	Location, size and extraosseous soft tissue component	E3—Needs contrast study to look for enhancement E4—Needs biopsy if associated with extraosseous soft tissue component

E1 category—normal examination or anatomical variant, E2 category—clinically unimportant finding, E3 category—likely unimportant, incompletely characterized, and E4 category—potentially important finding
CT computed tomography

Table 3 Tips and recommendations for incidentalomas in the extraspinal region

Extraspinal findings	Imaging and clinical evaluation	Category
Thyroid nodules	Assess for size, signs of adjacent infiltration and lymphadenopathy if any Further evaluation depends on size and lesion characters	E4—Further evaluation with FNAC/follow-up imaging depends on the size of the nodule and TIRADS category Heterogeneously enlarged thyroid gland needs US evaluation
Pulmonary nodules and masses	Usually detected on the localizers	E4—Identification of nodules and masses would require CT for further evaluation Follow-up is based on Fleischner Society guidelines
Hepatic lesions	Assess for lesion characteristics and predisposing factors for underlying primary malignancy	Prompt imaging, follow-up and possible biopsy in lesions with suspicious imaging features and high-risk individuals[a]
Adrenal lesions	Assess for lesion size and imaging findings	Prompt imaging, follow-up and possible biopsy in lesions with increased size and suspicious imaging features[a]
Renal lesions	Assess for the lesion size, solid/cystic nature, presence of internal septations/solid component/thick wall	Prompt imaging, follow-up and possible biopsy in lesions with suspicious imaging features and high-risk individuals[a]
Ovarian lesions	Assess for lesion size, solid/cystic nature, presence of internal septations/solid component/thick wall Further evaluation depends on patient age	Prompt imaging, follow-up and possible biopsy in lesions with suspicious imaging features and high-risk individuals[a]
Vascular lesions—aneurysms	Assess for location, branch vessel involvement and diameter	Follow-up depends on aneurysm size and associated risk factors with increased likelihood of rupture
Lymphadenopathy	Assess for size, homogeneous or heterogeneous signal intensity and contrast enhancement when available	Further evaluation depends on nodal size, number and suspicious imaging features; needs further evaluation to rule out underlying infectious etiology, metastatic lymphadenopathy and lymphoma[a]

CT computed tomography, *FNAC* fine needle aspiration cytology, *TIRADS* thyroid imaging, reporting and data system, *US* ultrasound
[a]Further evaluation depending on practice recommendations as described in the review

Fig. 1 Idiopathic syrinx. Sagittal (**a**) and axial (**b**) T2 weighted images show linear hyperintensity in the center of the spinal cord extending from C7 to D5 consistent with syrinx (*arrowheads*)

(<3 vertebrae) can be managed conservatively; compared to symptomatic patients with an extended syrinx (≥4 vertebrae), syrinx with underlying etiology or with progression on follow-up, which require surgical intervention [16, 17].

Ventriculus Terminalis

Ventriculus terminalis (VT) is a CSF-containing ependyma-lined cavity in continuity with the spinal canal involving the terminal cord, i.e., conus medullaris [18]. The VT is thought to be due to canalization and retrogressive differentiation [18]. It is usually seen on ultrasound and MRI in neonates and children with a prevalence of 2.6% with no related symptoms in children less than 5 years old, but rarely encountered in adults [19]; however, VT can be associated with congenital spinal dysraphism and Chiari malformation in children. Rarely, it can be secondary to trauma, hemorrhage and to a compressive or vascular pathology in adults [20–23].

The salient MRI findings include a cystic lesion involving the conus medullaris without associated altered cord signal intensity (Fig. 3). Uncommon findings include the presence of septations and cord edema [24]. Contrast medium administration helps to rule out an underlying malignancy in patients with unusual imaging findings.

When symptomatic, depending on clinical presentation, VT is classified into type 1A with nonspecific and stable neurological symptoms, type 1B with nonspecific and worsening symptoms, type 2 with focal neurological deficits and type 3 with sphincter dysfunction [25, 26]. Surgical management is reserved only for patients with worsening nonspecific symptoms, focal neurological deficits, and sphincter dysfunction, while those with stable nonspecific neurological symptoms are managed conservatively with close neurological and radiological follow-up.

Lipoma of the Filum Terminale

Lipoma of the filum terminale (LFT) is one of the commonest occult spinal dysraphisms [27]. It is encountered in approximately 1–5% of lumbar spine MRI scans and 5% of post-mortem biopsies [28–30]. It is believed to be a disorder of secondary neurulation where the arrested mesodermal cells differentiate into mature fat during the process of migration [29]. On MRI, it appears as a T1 and T2 hyperintense lesion within the thickened filum terminale with suppression on fat saturated images (Fig. 4). The MRI needs careful evaluation to rule out associated anomalies including low lying conus, tethered cord syndrome and vertebral abnormalities leading to scoliosis before designating LFT as a normal variant [30].

Asymptomatic LFT with or without low lying conus is usually managed conservatively unless associated with significant scoliosis, which can be a cause of spinal cord traction. Although prophylactic surgery in asymptomatic individuals remains controversial, symptomatic patients with tethered cord syndrome need surgical untethering [30].

CSF Flow Artifacts

The cerebrospinal fluid typically shows T1 hypointense and T2 hyperintense signal on MRI; however, due to its normal motion within the spinal canal, CSF is liable to artifacts on

Fig. 2 Hemangioblastoma. Sagittal T2 weighted image (**a**) shows dilated syrinx with a small nodule in the posterior wall (*arrowheads*) and cord hyperintensity adjacent to the syrinx (*arrow*). Axial gradient recalled echo image (**b**) shows syrinx with nodule in the posterior aspect which shows enhancement (*arrow*) on T1 post-contrast image (**c**) suggestive of tumor-associated syrinx

MRI which show a hypointense signal encircling the cord on axial images and are predominantly dorsal to the cord on sagittal T2 weighted images (Fig. 5; [31, 32]). The CSF-related artifacts on MRI can be grouped as time of flight (TOF) effects and those due to turbulent flow [33].

The TOF effects typically occur when the moving protons fail to experience both the initial radiofrequency pulse and the following refocusing pulse; more pronounced on spin-echo and fast spin-echo imaging. Due to laminar flow, these effects are more pronounced in the center. Conversely, peripherally moving protons are less prone to TOF effects due to lower velocity. The artifacts due to turbulent flow are due to lack of typical laminar flow caused by rapid dephasing and signal loss, commonly seen in the dorsal subarachnoid space of the thoracic spine on T2 weighted images, especially in children [34]. They can be avoided by changing the phase and frequency encoding direction [35]. Cross-referencing with other imaging planes and correlation with fast imaging sequences, such as gradient recalled echo, aid in accurate interpretation especially when they mimic a tumor or spinal vascular malformation.

Enhancement of Radicular Vein and Vein of Filum Terminale

The small perimedullary veins on the surface of the cord form the ventral and dorsal medial veins which drain into the epidural venous plexus through the great radicular and small radicular veins. In about 25% of the individuals, there is an accessory radicular vein which accompanies the filum terminale or dorsal lumbosacral nerve roots to drain into the epidural venous plexus. The increased caliber of veins ($\approx$1 mm) allows normal flow-related enhancement even in the absence of disc compression and spinal canal narrowing [34, 36, 37]. They are typically seen as curvilinear enhancement along the conus and filum terminale, to course along the nerve root and terminate in the neural foramen as they drain into the epidural venous plexus (Fig. 6). The awareness of normal venous enhancement helps avoid potential misdiagnosis as pathological inflammatory enhancement of the nerve roots [37].

Fig. 3 Ventriculus terminalis. Sagittal and axial T2W 3D *S*ampling *P*erfection with *A*pplication optimized *C*ontrasts using different flip angle *E*volution (SPACE) images (**a**, **b**) show a large ovoid lesion with signal intensity similar to CSF causing expansion of the conus medullaris (*arrows*). The lesion shows lack of contrast enhancement on sagittal T1 weighted image (*arrowhead*) suggestive of benign etiology

Perineural and Meningeal Cysts

Meningeal cysts are outpouchings of the subarachnoid space, which can be either extradural and lined by arachnoid layer or intradural in location forming a leptomeningeal cyst. Meningeal diverticula are true outpouchings from the meninges which can be either in the midline, commonly in the sacral region, or along the spinal nerve root proximal to the dorsal root ganglion forming a spinal nerve root diverticulum (Fig. 7; [34, 38, 39]).

Extradural meningeal cysts are outpouchings of subarachnoid space through the dura and can arise anywhere along the thecal sac. Extradural arachnoid cysts commonly involve the dorsal cord and communicate with the subarachnoid space adjacent to the entry of the dorsal nerve root. Spinal nerve root diverticula are outpouchings of the subarachnoid space with a dural lining, commonly involving the lower cervical, lower lumbar and upper sacral regions. Dilated nerve root sheaths are prolongations of the subarachnoid space along the nerve sheath, a normal variant which should not be misdiagnosed as a post-traumatic pseudomeningocele, which characteristically shows absence of the nerve root.

Perineural cysts (Tarlov cysts) are CSF-containing lesions in the extradural space at the junction of the dorsal nerve root ganglion and posterior nerve root [38, 40]. These cysts contain the neural tissue within the cavity or in the walls of the cyst with possible microcommunication with the CSF in the subarachnoid space. Perineural cysts are common (although not reported), with a reported imaging incidence of 1–5% of which approximately 25% are believed to cause symptoms [41–43]. They may present insidiously due to a gradual increase in size or present initially with sacrococcygeal pain, pain along the nerve root distribution or bladder and bowel disturbances [44]. These lesions show varied appearance ranging from simple rounded cyst to a multiloculated cystic lesion in the neural foramen and may be associated with erosion and widening of the sacral foramina (Fig. 8). Perineural cysts with atypical findings such as a complex loculated cystic mass, post-contrast enhancement, presacral location, and pelvic extension need careful evaluation as they mimic nerve sheath tumors, such

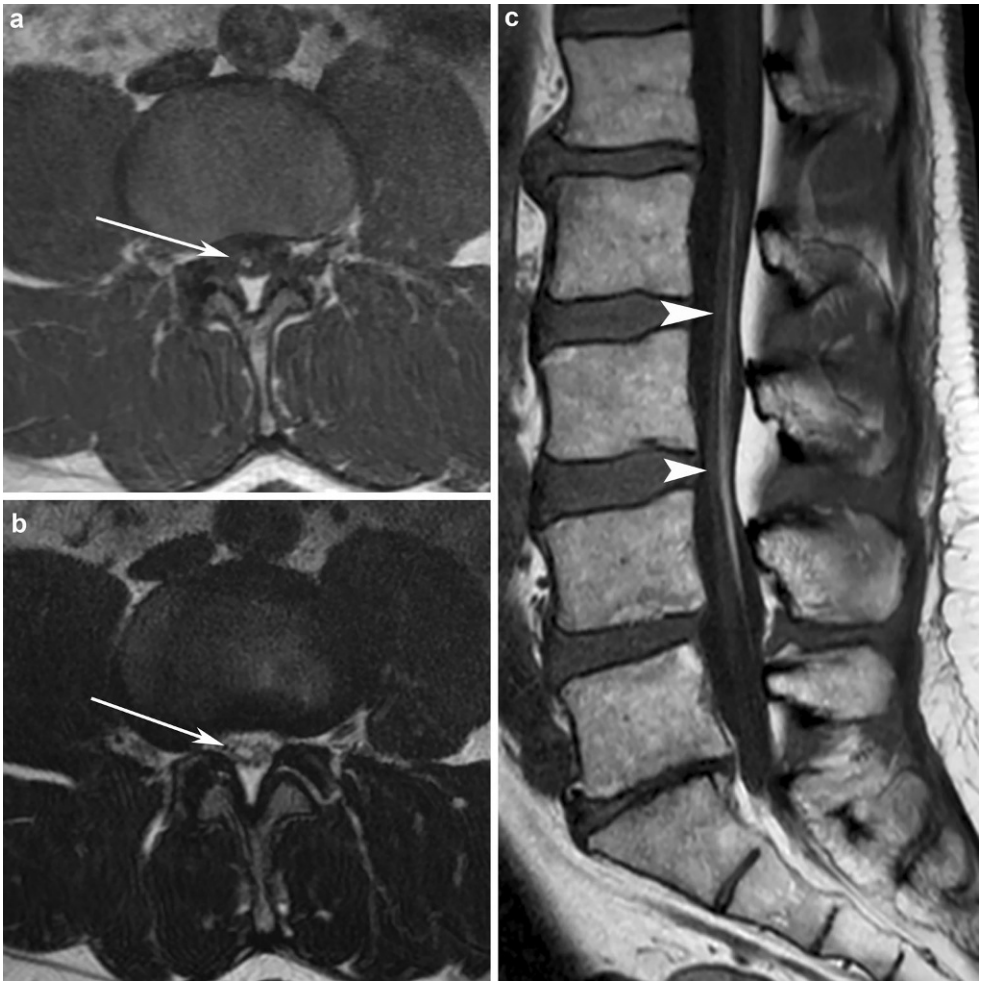

Fig. 4 Lipoma of the filum terminale. Axial T1 and T2 weighted images (**a**, **b**) show a hyperintense lesion (*arrows*) extending along the nerve roots from the level of L2 to L5 vertebral bodies (*arrowheads*) as seen on sagittal T1 weighted image (**c**) suggestive of lipoma

as schwannoma or neurofibroma, dural ectasia, meningocele or endopelvic cystic masses [45, 46].

Despite the risk of an increase in size along with delayed presentation, asymptomatic lesions are rarely reported [43]. Symptomatic cysts could be managed using CT guided aspiration and fibrin sealant injection as an initial treatment option with surgical management reserved for those with recurrence or failure to show improvement post-aspiration [41, 43].

Incidentalomas in the Vertebral Body and the Posterior Arch

The IFs involving the vertebral body and the posterior arch include mild congenital vertebral abnormalities, anatomical variants and benign bone tumors which are generally asymptomatic.

Congenital Vertebral Abnormalities

The spine and spinal cord are associated with abnormalities and variations due to disruption in any stage of the sequential development. Although severe abnormalities are symptomatic and lead to deformity, minor ones are usually asymptomatic and are detected fortuitously. This section deals with common incidentally detected abnormalities among a myriad spectrum and are grouped on an embryological basis.

Defective Vertebral Segmentation

Block Vertebra

These abnormalities are due to failure of segmentation of the somites with resultant congenital fusion involving either the ventral (the vertebral body), dorsal (the posterior arch) or both elements (Fig. 9). They commonly occur at the level of the cervical spine and in association with Klippel-Feil syndrome [47]. The fusion might lead to accelerated degeneration of the adjacent discs. Identification of congen-

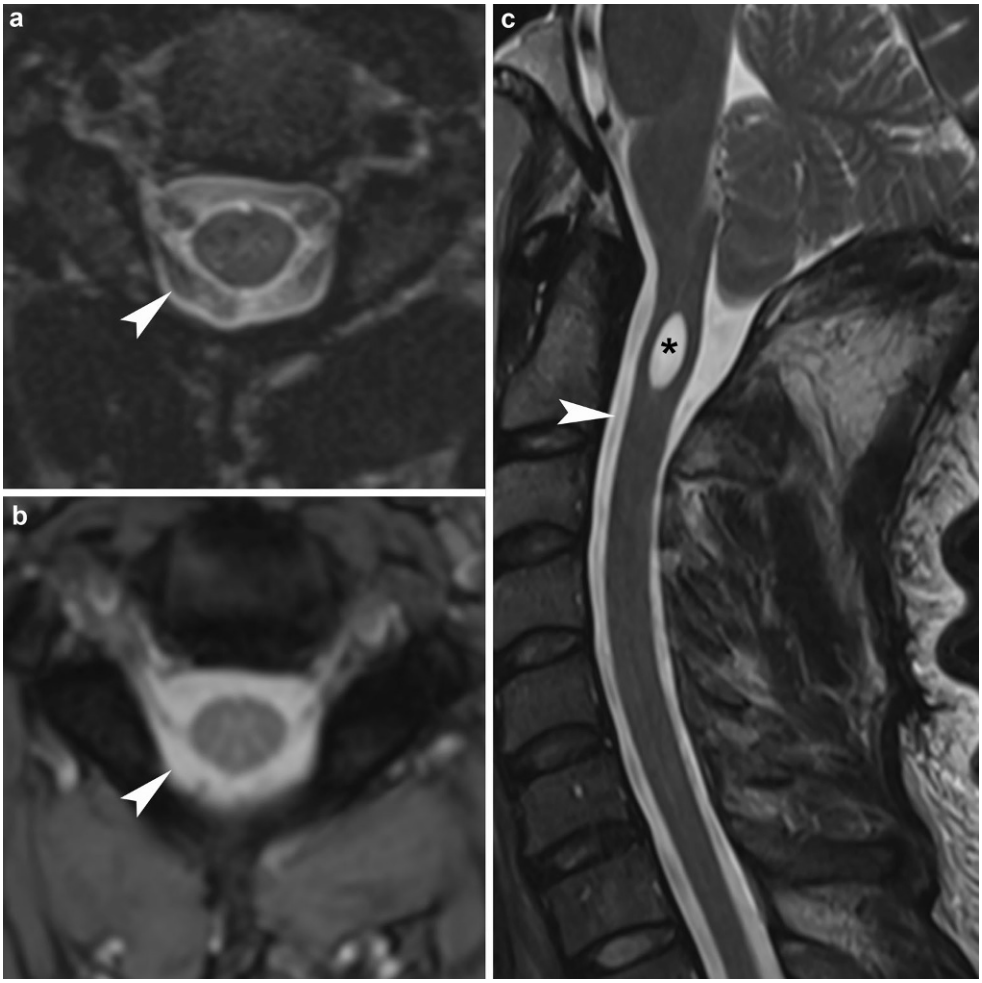

Fig. 5 CSF flow artifact. Axial T2 weighted image (**a**) shows hypointensity in the subarachnoid space (*arrowhead*) encircling the spinal cord. This is also seen on T2 weighted image (**c**) anterior (*arrowhead*) and posterior to the cord. The short TE on gradient recalled echo (**b**) eliminates the flow artifact (*arrowhead*) around the spinal cord. Notice the inferiorly located peg-shaped cerebellar tonsils with syrinx (*asterisk*) in the cervical cord at the level of C2 consistent with Chiari type 1 malformation

ital fusion should alert the radiologist to look for abnormalities such as Sprengel deformity and omohyoid vertebra along with a systematic evaluation for associated cardiac and genitourinary abnormalities in Klippel-Feil syndrome [48].

Disorders of Sclerotomal Fusion, Chondrification or Ossification

Butterfly Vertebra

Butterfly vertebrae are due to the failure of fusion involving the ventral sclerotomal pairs resulting in either a sagittal cleft or midsagittal constriction (Fig. 10). Although usually asymptomatic, accurate identification is important as they can be mistaken for wedge compression fractures on sagittal images [49]. A sclerotic border along the midsagittal cleft or constriction is diagnostic of butterfly vertebra.

Congenital Abnormalities of C1

Abnormalities of the posterior arch of C1 are thought to be due to abnormal chondrification whereas the defects of the anterior arch are possibly secondary to trauma [50, 51]. Posterior arch abnormalities are more common and are classified into five subtypes i. e., type A failure of posterior arch fusion in the midline, type B unilateral defects, type C bilateral defects, type D absence of the posterior arch with persistent tubercle and type E absence of the entire arch including the tubercle with type A being the most common subtype (Figs. 11 and 12; [52, 53]). The prevalence of congenital abnormalities of C1 is variable, ranging from 1% to 5.6% [53, 54]. Although most of these abnormalities are asymptomatic, they can lead to myelopathy, early degeneration of the cervical spine and may lead to cervical instability. Similar to butterfly vertebra, recognition of the corticated and smooth margin is necessary to avoid misdiagnosis/treatment as fractures or marrow infiltrating pathology such as metastasis [55].

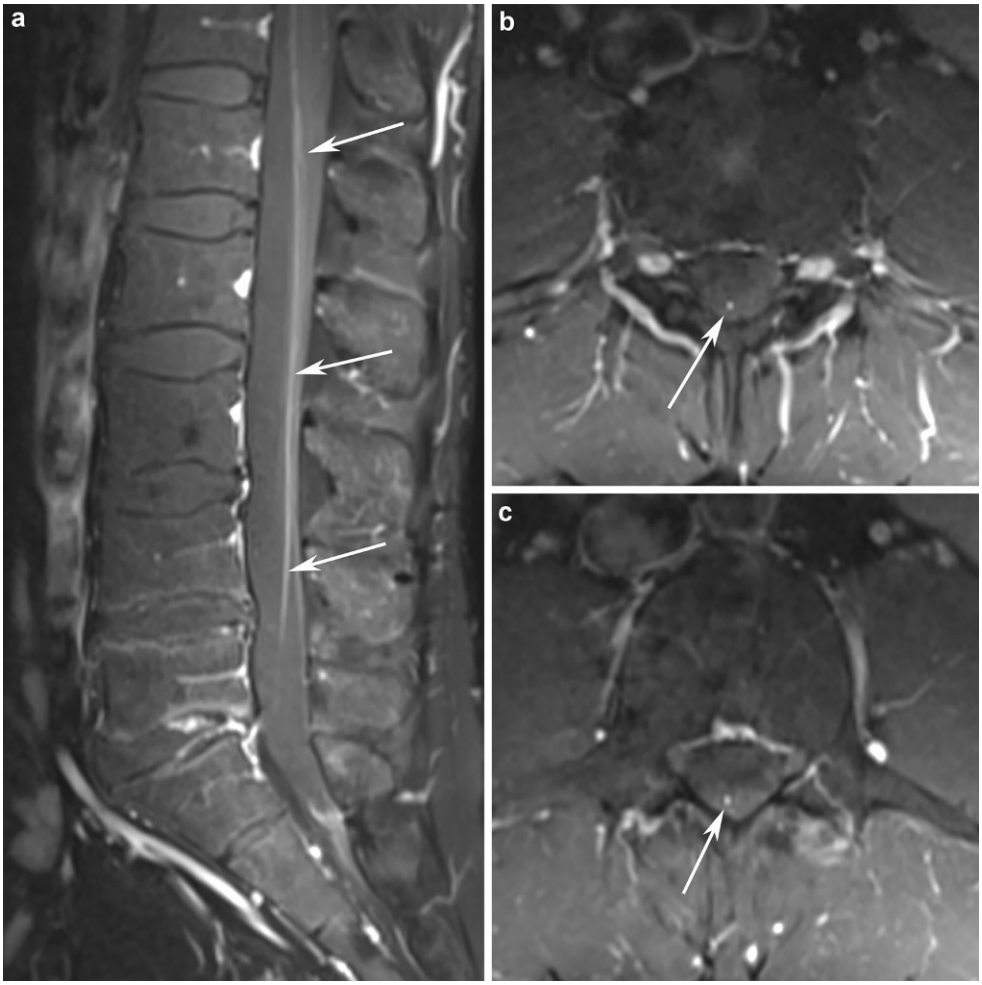

Fig. 6 Radicular vein. Sagittal (**a**) and axial (**b**, **c**) T1 fat saturated post-contrast images show a linear enhancing structure (*arrows*) coursing along the nerve roots consistent with a great radicular vein

Craniovertebral Junction Abnormalities

Os Odontoideum

An os odontoideum is a well-defined, rounded odontoid process with corticated margins unfused with the body of C2. There are two subtypes, orthotopic and dystopic types which can be stable or unstable [56]. It can be associated with Klippel-Feil syndrome, Down syndrome and Morquio's syndrome. The unstable variety can be symptomatic and need surgical intervention. As described, it can be associated with cervical instability and predispose the individuals to spinal cord injury, cervical stenosis, and chronic progressive myelopathy.

Ossiculum Terminale

Persistent ossiculum terminale results from failure of fusion of the secondary ossification center (at the tip of the dens) with the body of C2. Usually and similar to os odontoideum, ossiculum terminale is an incidental finding but can be misdiagnosed as a dens fracture. The presence of smooth, corticated margins enables differentiation between the two entities.

Developmental Variants

These include thoracolumbar junction variance and lumbosacral transition vertebra. Misdiagnosis of a transitional vertebra could lead to errors in numbering the lumbar vertebrae and the discs with a subsequent risk of consequent inapt surgical intervention [57].

Benign Bone Tumors

Vertebral Hemangioma

Vertebral hemangiomas (VH) are the most common benign tumors of the spine. The incidence increases with age, most commonly in the fourth or fifth decades of life. A VH occurs most commonly in the thoracic spine, followed by the lumbar spine and rarely in the cervical and sacral spine [58]. Typical VHs show high adipocyte content and are poorly vascular, as opposed to atypical and aggressive

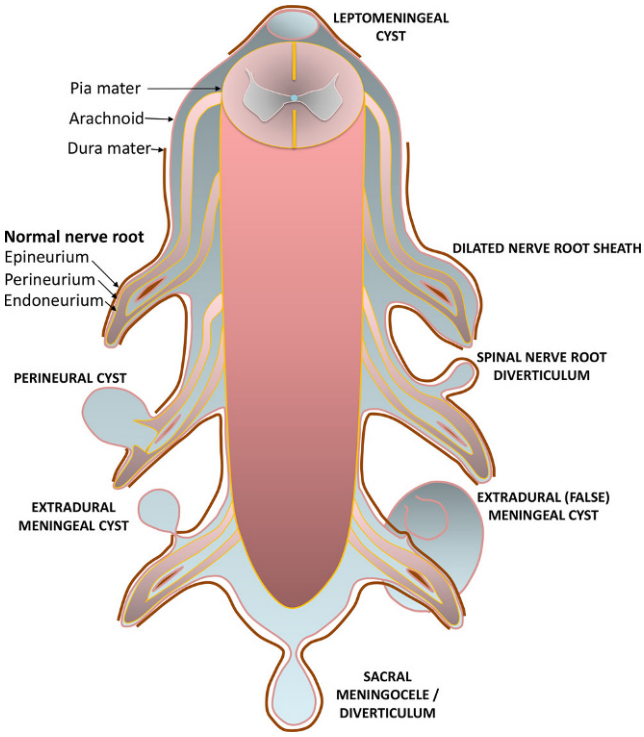

Fig. 7 Spinal meningeal cysts (adapted from Tarlov et al. [38]). Perineural cyst (*middle left*) occurring at the junction of the dorsal root ganglion and posterior root, containing neural tissue and lined by arachnoid. Meningeal cysts (*right, superior in midline*): an outpouching of subarachnoid space, which can be extradural (*lower left*), intradural (*top in midline*) and secondary to rupture of pre-existing extradural meningeal cyst (*lower right*). Meningeal diverticulum occurring in the midline, i.e. sacral meningocele (*bottom in midline*) and along the nerve root proximal to the dorsal root ganglion forming spinal nerve root diverticulum (*middle right*). Dilated nerve sheath (*top right*) which is a normal variant consisting of prominence of the subarachnoid space along the nerve root

VHs which show less fat component and higher vascular content. Typically, VHs show sparse thickened bony trabeculae with adjacent hypodense stroma producing a characteristic polka dot appearance on axial CT images. Due to the vertical orientation of the thickened bony trabeculae, they show corduroy appearance on sagittal and coronal images. The predominance of the fat component is reflected in the T1 and T2 hyperintense signal along with a well-defined nature, mild hyperintensity on inversion recovery sequences and variable enhancement on postcontrast sequences. There are interspersed areas of punctate and linear T1 hypointensity within the hyperintense lesion reflecting thickened trabeculae (Fig. 13). In comparison, atypical VHs show isointense to hypointense signal on T1 and hyperintense signal on T2 and inversion recovery sequences due to less fat and higher vascular content along with variable enhancement on postcontrast sequences. Although rarely seen, the presence of thickened bony trabeculae on CT and MRI is a diagnostic feature in atypical VHs. The presence of extraosseous soft tissue, epidural and neural foraminal component causing spinal cord and nerve root compression and enlarged paraspinal vessels with or without posterior arch involvement should suggest aggressive hemangioma (Fig. 14; [59]). In the absence of thickened bony trabeculae, advanced MRI aids in differentiating atypical VHs from metastasis. Atypical VHs show a more pronounced drop in signal on chemical shift imaging, higher apparent diffusion coefficient (ADC) values on diffusion-weighted imaging, and lower plasma volume and permeability perfusion parameters compared to metastasis [60, 61].

The vast majority of VHs are asymptomatic lesions, incidentally found on imaging studies [62]. Rarely, VHs display aggressive behavior and are symptomatic (approximately 1% of cases). Although asymptomatic VHs are managed conservatively, symptomatic ones may need percutaneous procedures such as vertebroplasty or transarterial embolization, radiotherapy, surgery or a combination of these [59].

Bone Island/Enostosis

Enostoses are benign bony lesions characterized by the presence of cortical bone within the cancellous bone. They are thought to be due to abnormal endochondral ossification causing failure of resorption of cortical bone leading to hamartomatous cortical bone. The estimated prevalence of enostosis in the spine is approximately 1% but could be as high as 14% [63, 64]. These lesions show dense sclerosis with a typical rim of brush-like spiculations on CT, low signal intensity on T1 and T2 weighted imaging with lack of enhancement on postcontrast imaging, and lack of activity compared to normal bone marrow on scintigraphy and positron emission tomography (PET) studies (Fig. 15; [65]). Dense sclerosis with brush-like spiculations (>1060 HU) on CT and hypoactivity on scintigraphy studies enable differentiation from osteoblastic metastasis [66].

Clinically, enostoses are IFs, mostly asymptomatic and leave alone lesions.

Benign Notochordal Cell Tumor

Benign notochordal cell tumors (BCNT) are benign, intraosseous lesions of notochordal origin. They are also called giant notochordal rests, hamartomas or benign chordomas. They are seen in midline structures in approximately 20% of autopsy series commonly involving the sacrococcygeal vertebrae (12%) and clival region (11.5%) [67]. They share a similar anatomical region as malignant chordomas and need to be differentiated from chordomas or metastases as the latter are aggressive and have a clinically poor prognosis. The BCNTs are usually small with preserved bony architecture and sclerosis on CT, show hypointense signal on T1, hyperintense signal on T2

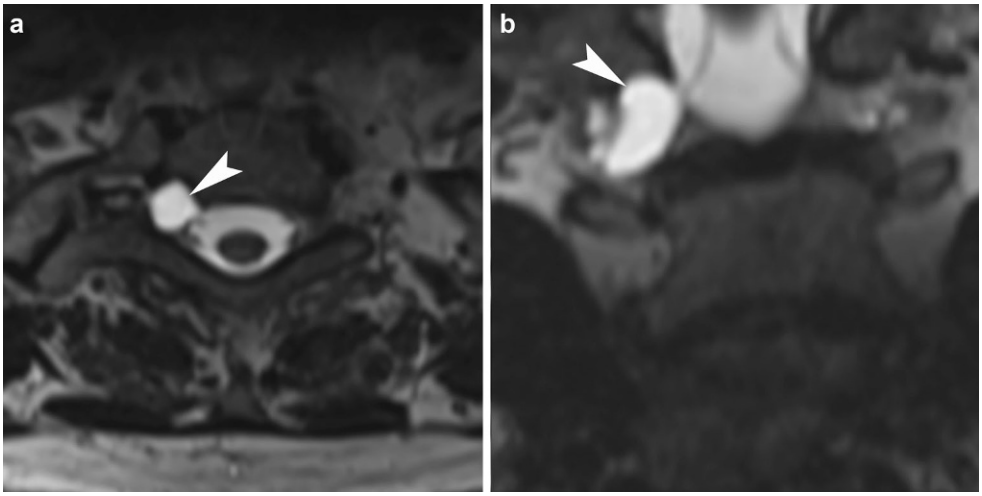

Fig. 8 Perineural cyst. Axial (**a**) and coronal (**b**) T2 SPACE image shows a T2 hyperintense lesion in the neural foramen on the right side (*arrowhead*) in relation to the exiting nerve suggestive of a perineural cyst

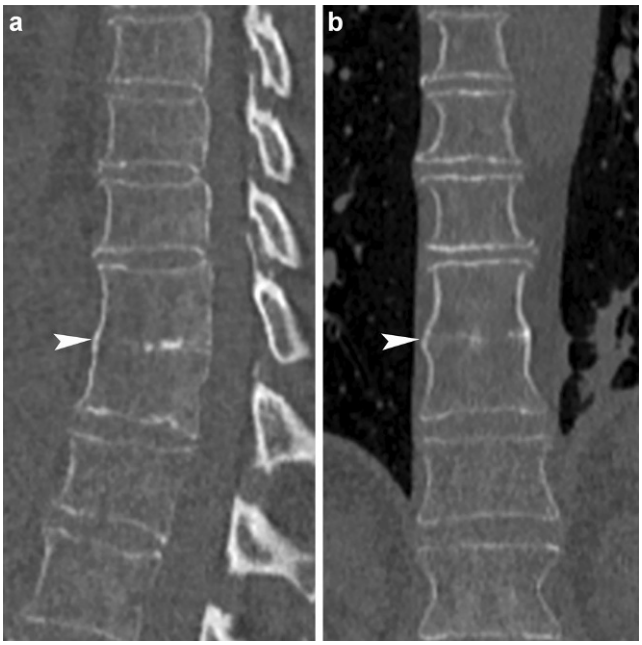

Fig. 9 Block vertebra. Sagittal (**a**) and coronal (**b**) CT images in bone window show fusion of lower dorsal vertebral bodies with absence of intervertebral disc (*arrowhead*) suggestive of block vertebra

and absence of postcontrast enhancement (Fig. 16). They are usually intraosseous with the absence of extraosseous soft tissue components. Chordomas, on the contrary, are large aggressive lytic lesions with extraosseous soft tissue component. They show a similar signal intensity on MRI with characteristic postcontrast enhancement which enables differentiation from BCNTs [68, 69].

The BCNTs are usually asymptomatic but can present with back pain in some cases. Although some reports suggest coexistence with chordomas and the possibility of BCNTs being a prechordomatous condition, there is little evidence to support this hypothesis [70]. Currently, conservative management with periodic follow-up is suggested. If suspicion of a malignant tumor exists, image-guided biopsy should be performed.

Incidentalomas in the Extraspinal Region

Extraspinal incidentalomas that can be visualized on CT and MRI of the spine are numerous and spinal imaging is barely optimal for complete diagnosis as they are usually non-contrast enhanced studies and are tailored for adequate evaluation of the spinal cord, vertebral bodies, and the posterior arch. The analysis of spine CT should include evaluation of both limited field of view (FOV) spine images and full FOV chest/abdomen images to avoid a potentially overlooked diagnosis as full FOV images are usually needed for optimal evaluation of extraspinal abnormalities [71]. Using saturation bands on MRI obscures visualization of prevertebral structures and might be insufficient for optimal diagnosis of obvious prevertebral pathology. The detailed description of extraspinal findings is beyond the scope of this review. Since it is necessary for the radiologist to know the available practice recommendations for further evaluation and the management framework of extraspinal incidentalomas when identified, the article focuses briefly on the recommendations which are not absolute guidelines and can be modified on an individual basis.

Thyroid Findings

Thyroid nodules are the most common extraspinal findings on cervical spinal MRI [6, 7]. They show either homogeneous or heterogeneous appearance usually with isointense signal on T1 and hyperintense signal on T2 weighted images (Fig. 17; [72]). The presence of hyperintense signal on T1 weighted images suggests colloid degeneration or hemorrhage. As there are no reliable findings to differen-

Fig. 10 Butterfly vertebra. Coronal CT image in bone window (**a**) shows a midline constriction in the D4 vertebral body mimicking posterior wedging on sagittal image (**b**). Cinematic rendered image (**c**) shows better depiction of butterfly vertebra

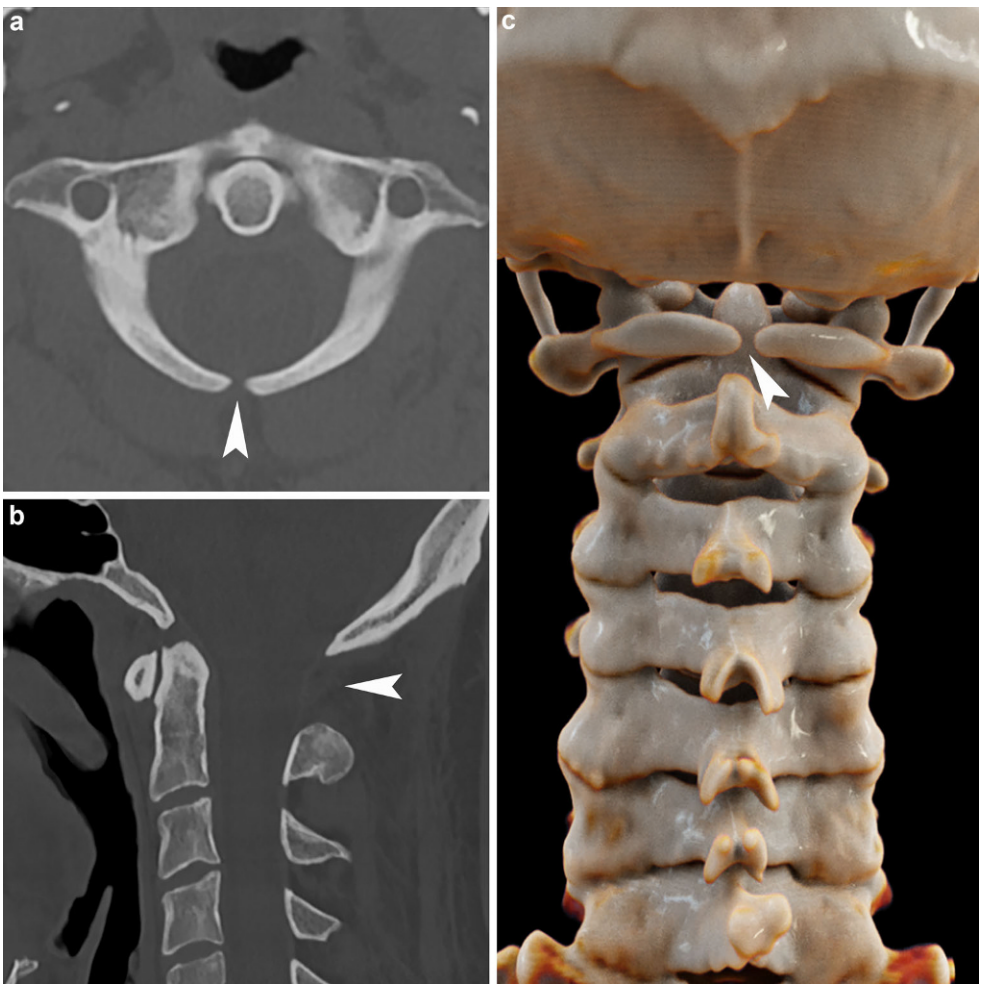

Fig. 11 Type A abnormality of posterior arch of C1. Axial (**a**) CT image in bone window shows non-fusion of the posterior arch of C1 in the midline with corticated margins (*arrowhead*). Midsagittal (**b**) CT image shows nonvisualization of posterior arch as depicted by bony defect on cinematic rendered image (*arrowhead*) (**c**)

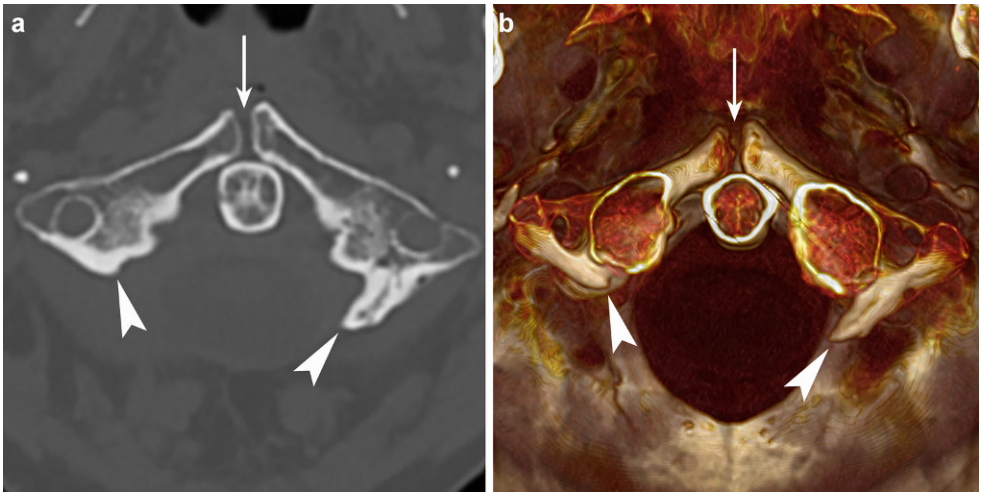

Fig. 12 Combined abnormalities of C1 arch. Axial (**a**) CT image in bone window and 3D volume rendered image (**b**) show complete absence of the posterior arch with absence of the tubercle (*arrowheads*) with unfused anterior arch (*arrow*)

Fig. 13 Typical vertebral hemangioma. Axial (**a**) and coronal (**b**) CT images in bone window show prominence of bony trabeculae (polka dot sign) in axial and corduroy sign in coronal sections (*arrows*). Sagittal T1 (**c**) and T2 (**d**) weighted images show hyperintense signal (*arrowhead*) involving the T10 vertebra

tiate benign from malignant nodules on imaging, size is the only criterion which guides further evaluation. Nodules should be evaluated for suspicious features including abnormal lymph nodes and invasion of adjacent structures, which is unlikely in an asymptomatic nodule. Any nodule with suspicious features needs further evaluation with ultrasound and fine needle aspiration cytology. The recent Thyroid Imaging, Reporting and Data system (TIRADS) classification evaluates nodules based on their characteristics on ultrasound. A thyroid nodule is assessed for composition, echogenicity, shape, margins and presence of echogenic foci and classified into 5 categories including TR1 (be-

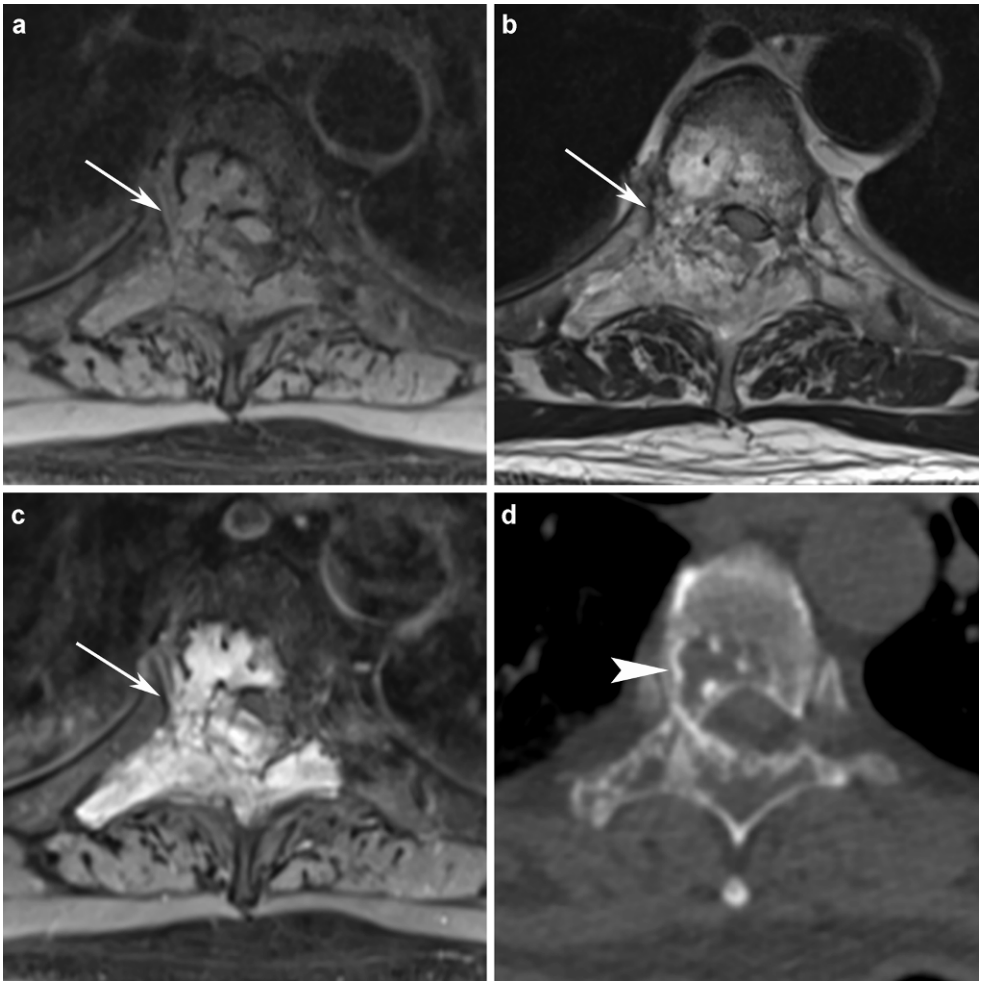

Fig. 14 Aggressive hemangioma. Axial T1 fat saturated (**a**), T2 (**b**) and T1 fat saturated post contrast (**c**) images show hyperintense lesion involving the T5 vertebral body, right pedicle and posterior arch with epidural component and cord compression, displacement and enhancement (*arrow*). Axial CT image in bone window (**d**) shows bony erosion and prominent vertical trabeculations (*arrowhead*) suggestive of aggressive hemangioma

nign), TR2 (not suspicious for malignancy), TR3 (mildly suspicious for malignancy), TR4 (moderately suspicious for malignancy) and TR5 (highly suspicious for malignancy). Accordingly, fine needle aspiration cytology is suggested for TR3 lesions >2.5 cm, TR4 lesions >1.5 cm and TR5 lesions >1 cm along with follow-up imaging for TR3 lesions >1.5 cm, TR4 lesions >1 cm and TR5 lesions >0.5 cm. Heterogeneous, enlarged thyroid glands found incidentally in patients without serious comorbidities or limited life-expectancy need further evaluation with ultrasound [73].

Pulmonary Nodules and Masses

Spinal imaging is grossly inadequate for evaluating pulmonary nodules and masses due to the limited FOV, which is focused on the vertebral and paravertebral region. The identification of pulmonary lesions on spinal imaging usually takes place on the inspection of localizers used to plan thoracic spine MRI. Even though MRI suffers from limitations due to low proton density and increased susceptibility artifacts at tissue-air interfaces, lesions with increased tissue attenuation such as pneumonia or tuberculosis, as well as benign or malignant tumors can be identified on MRI [74]. Pleural effusion was the most common incidental finding in previous studies evaluating thoracic spinal imaging and cardiac MRI [7, 75]. A dedicated imaging protocol can achieve a sensitivity of 75–90% for nodules with sizes between 4–8 mm and 100% for nodules >8 mm [76]. These lesions would require prompt CT evaluation and follow-up based on the Fleischner Society recommendations for incidental pulmonary nodules [77].

Hepatic Lesions

Hepatic incidentalomas were seen in 0.2–1.8% of individuals on lumbar spine imaging. Of these, 0.15–0.5% showed hepatic cysts and 0.6–0.9% of individuals had hepatic masses or unclassified T2 hyperintense lesions [4–7]. Further work-up depends primarily on the size, presence of underlying predisposing factors (e.g. cirrhosis, non-alcoholic steatohepatitis, hemochromatosis, primary sclerosing cholangitis), which increase the likelihood of an incidental lesion being a primary malignancy. Likewise, the presence of an underlying malignancy will increase the

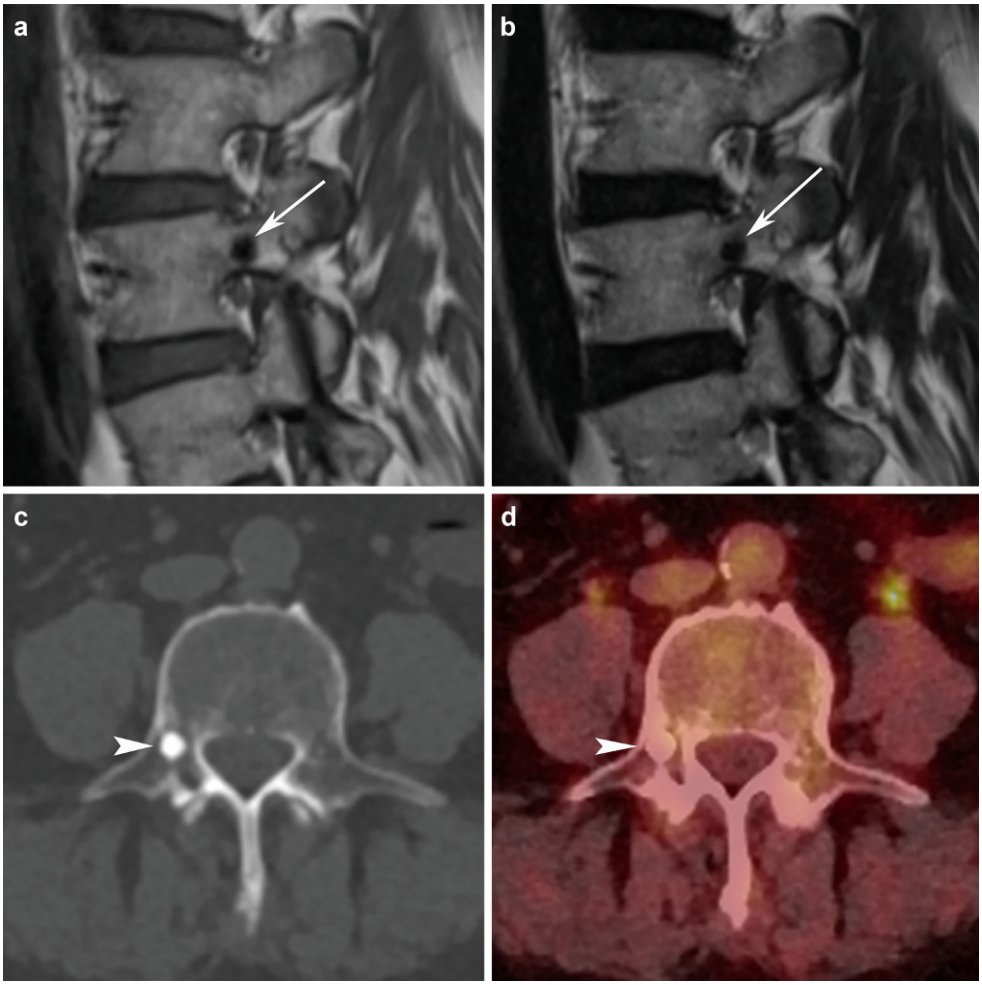

Fig. 15 Bone island. Sagittal T1 (**a**) and T2 (**b**) weighted images of lumbar spine show well defined hypointense lesion involving the pedicle of L4 on the right side (*arrows*). Axial CT (**c**) and PET-CT (**d**) images show a sclerotic lesion with lack of activity on PET-CT (*arrowhead*)

likelihood of an incidental lesion being a liver metastasis [78, 79]. The current recommendations for incidental findings are for lesions identified on CT. Although MRI of the spine can reliably diagnose a benign cyst in the hepatic parenchyma, adequate evaluation of a solid or complex cystic lesion showing altered signal intensity would need contrast-enhanced multiphase hepatic protocol CT or MRI.

The imaging evaluation should focus on suspicious features including ill-defined margins, heterogeneity, mural thickening, nodularity or thick septations and enhancement patterns in arterial, portal and equilibrium phases of the postcontrast study (dubious in spine imaging), whenever available. Any lesion <1 cm in a low-risk patient is considered benign and does not need further evaluation. It does however require a follow-up MRI scan in 3–6 months in a high-risk individual for characterization and interval growth. Lesions between 1 cm and 1.5 cm with benign imaging appearance need no further follow-up, whereas lesions with suspicious imaging features in both low and high-risk individuals require prompt MRI evaluation. Similarly, lesions >1.5 cm with suspicious features require prompt MRI alone in low-risk individuals and prompt MRI with biopsy in high-risk individuals [80].

Adrenal Lesions

Adrenal incidentalomas are uncommon, accounting for approximately 0.1–0.8% of patients evaluated for lumbar spine pathology (Fig. 18; [4, 5]). Benign adrenal adenomas are the most common adrenal masses in patients with no known malignancy and, owing to their high prevalence, an incidental adrenal lesion encountered in a cancer patient is also likely to be of benign etiology [81, 82]. The size, previous history of malignancy and the presence of benign imaging features guide future imaging recommendations in patients with adrenal incidentalomas. Any lesion <1 cm in size and those which are predominantly fatty with low attenuation on non-contrast CT (<10 HU) and signal loss on chemical shift MRI are deemed benign, regardless of size; however, in lesions with no definite benign imaging features, further evaluation is recommended. Lesions measuring 1–2 cm in size need follow-up imaging with an adrenal CT protocol to look for interval growth. Lack

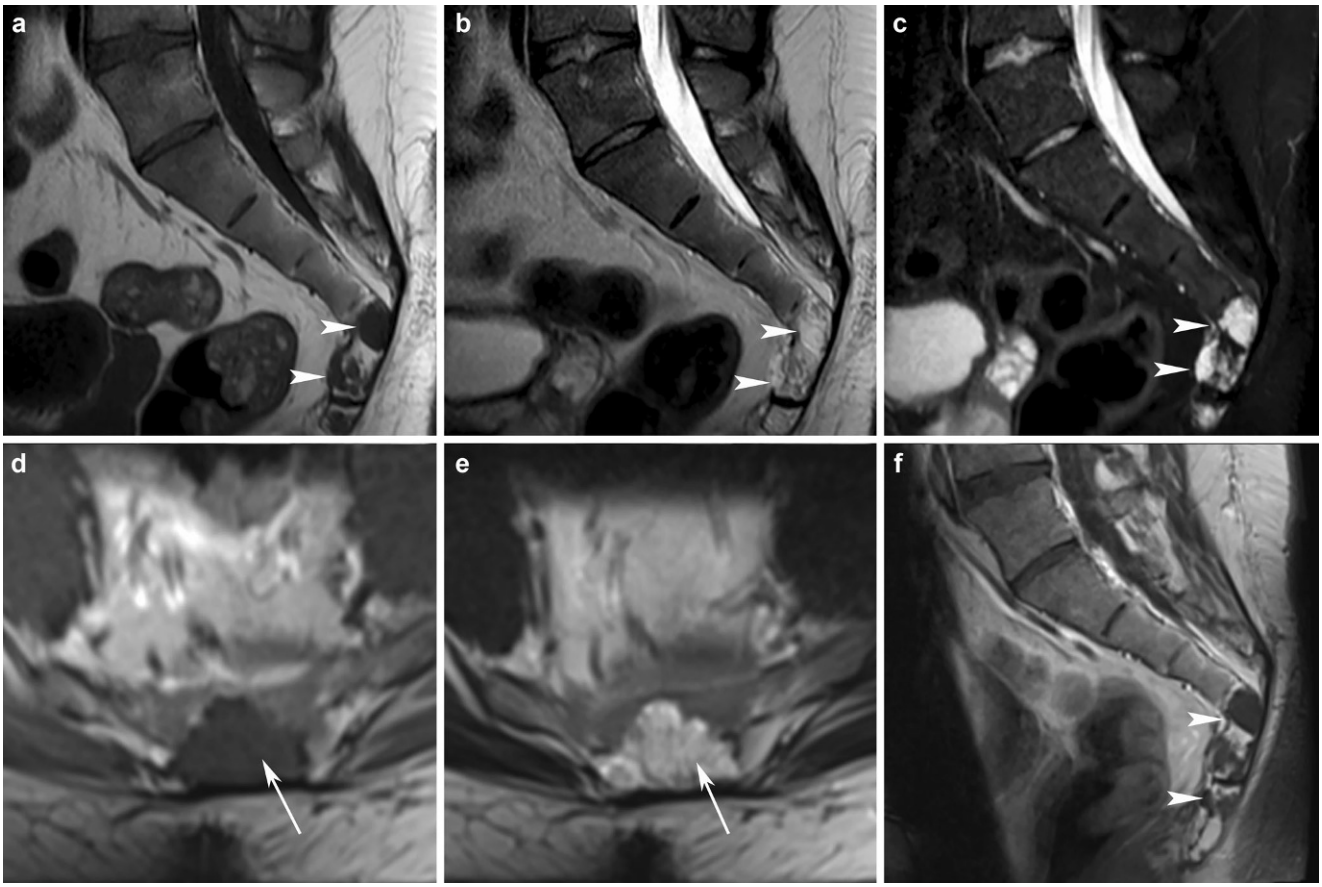

Fig. 16 Benign notochordal cell tumor. Sagittal T1 (**a**), T2 (**b**) and STIR (**c**) images show T1 hypointense, T2 and STIR hyperintense lesion (*arrowhead*) involving the S4 and S5 sacral vertebrae. The lesion is well visualized on axial T1 (**d**) and T2 (**e**) weighted images with no evidence of contrast enhancement on sagittal T1 postcontrast image (**f**; *arrow*), characteristic of benign notochordal cell tumor

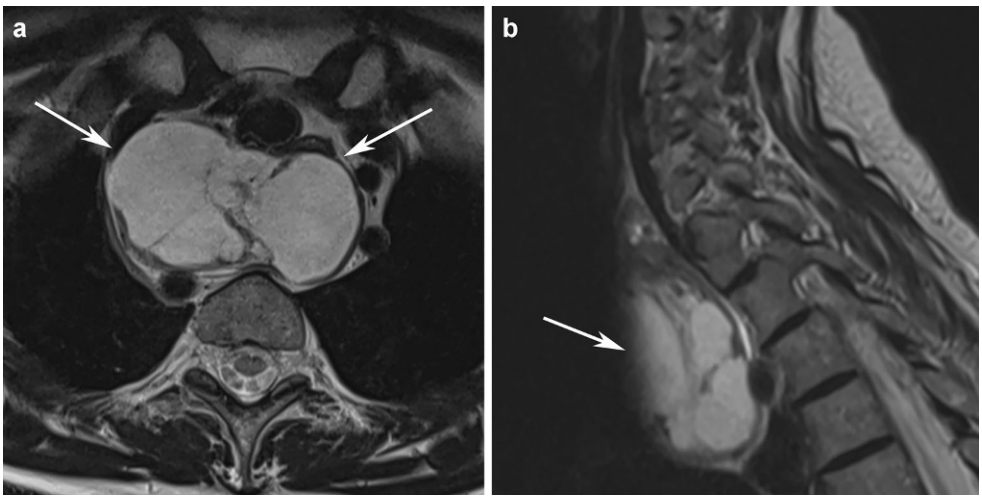

Fig. 17 Retrosternal goiter. Axial (**a**) and sagittal (**b**) T2 weighted images of cervical spine show a well-defined multiseptated lesion arising from the inferior aspect of the right lobe of the thyroid (*arrows*) with retrosternal extension and displacement of the esophagus confirming retrosternal goiter

of interval growth on follow-up imaging for more than 1 year or on comparison with previous imaging would suggest a benign lesion. For lesions between 2–4 cm, further imaging with prompt adrenal CT is recommended. In an unlikely scenario where a definite diagnosis cannot be reached, follow-up imaging after 6–12 months may be needed. In patients with known malignancy, adrenal lesions showing central necrosis might need biopsy or PET-CT to rule out metastasis. Lesions >4 cm in size without definite benign diagnostic features in patients with a history of malignancy and in cases where adrenocortical carcinoma

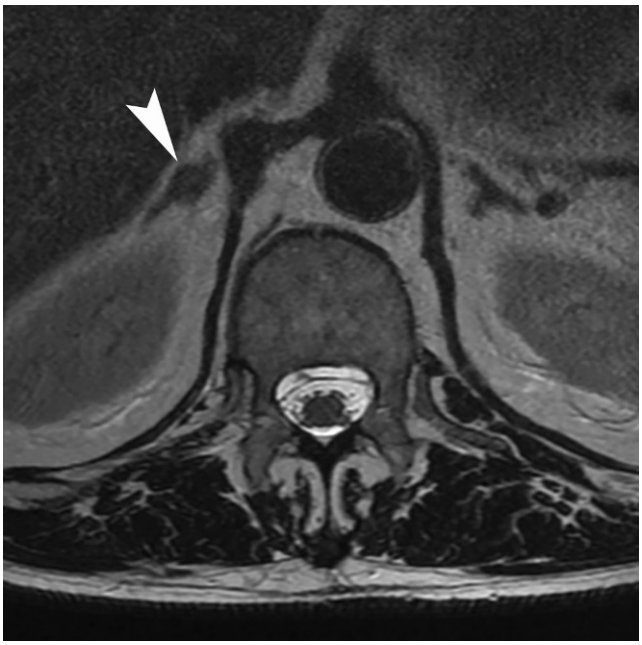

Fig. 18 Adrenal adenoma. Axial T2 weighted image shows an incidental adrenal nodule (<1 cm) involving the body of the right adrenal gland, which needs no further evaluation (*arrowhead*)

is strongly suspected, surgical removal (without biopsy) is recommended [83].

Renal Lesions

Renal incidentalomas are one of the most commonly encountered lesions in lumbar spine imaging ranging between 6.2% and 27.2% with renal cysts being most common in 6.4–24.4% of individuals and renal mass lesions in approximately 0.16% of individuals [4–7]. The use of CT and MRI of the spine with limited FOV is suboptimal for evaluation of small solid renal lesions, and larger ones are better appreciated due to altered external contour; however, cystic renal lesions are easily seen due to innate hyperintense signal on T2 weighted imaging (Fig. 19). An increase in size of solid lesions and increased complexity of cystic lesions correlate with malignant potential. Any lesion with suspicious imaging features would need contrast-enhanced multiphase renal protocol CT for further evaluation. The Bosniak classification is routinely used for evaluation and further management recommendations in cystic renal lesions. Bosniak type I and II cysts are benign without any need for follow-up imaging. Bosniak type IIF cysts with thin septations and mildly thickened wall with no appreciable enhancement need follow-up imaging. Recent recommendations suggest initial biannual imaging with annual imaging then on for 5 years to look for morphological changes suggesting malignancy. Bosniak type III and IV cysts need treatment due to an increased likelihood of malignancy [84]. Size and the presence of calcifications are no longer significant factors in the Bosniak classification [85]. Solid lesions <1 cm require the same follow-up as Bosniak type IIF cysts. Stable lesions need no follow-up. Solid lesions without fat which are <1 cm, those that show interval change, and those measuring 1–4 cm and >4 cm in size need a biopsy or further management [86]. Solid lesions which are predominantly fatty and that typically lack calcification (i. e., angiomyolipomas) need further management if they are larger than 4 cm or if they contain intralesional aneurysms larger than 0.5 cm.

Pelvic Lesions

Pelvic incidentalomas are myriad, usually encompassing bowel lesions, uterine and ovarian lesions in females along with prostatic and seminal vesicle pathologies in males. Uterine myomas are seen incidentally in 1.7–7.3%, cystic uterine lesions (e. g., Nabothian cysts) in 0.5–3.7%, ovarian cystic lesions in 2.2–7.3%, ovarian solid lesions in 0.2%, colonic diverticulosis in 0.08–11.7% and colorectal wall

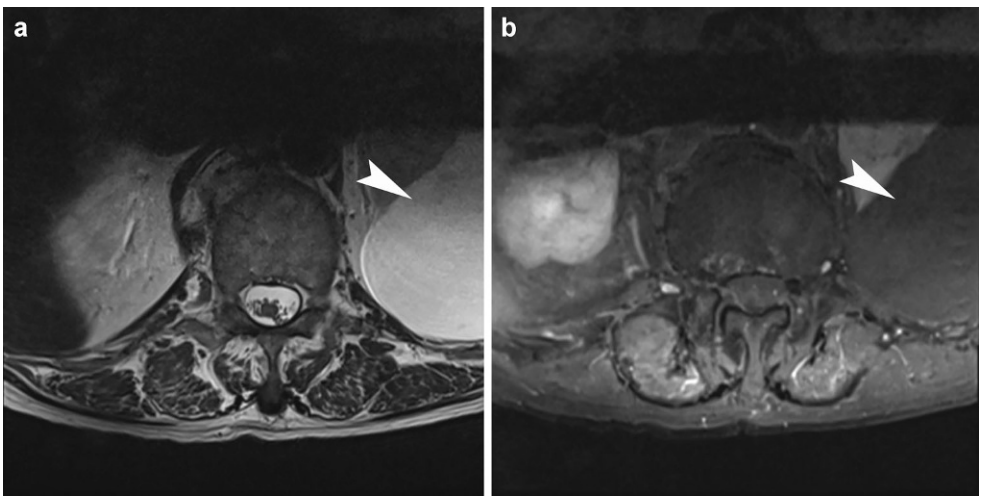

Fig. 19 Simple renal cyst. Axial T2 (**a**) and T1 fat saturated postcontrast (**b**) images show well-defined T2 hyperintense lesion (*arrowhead*) which lacks postcontrast enhancement

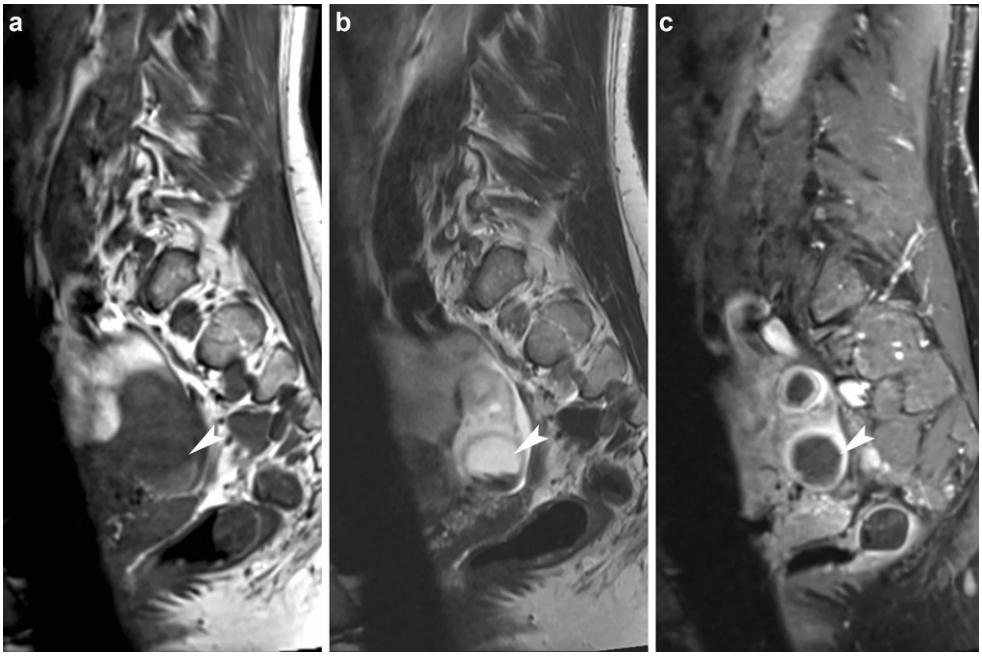

Fig. 20 Hemorrhagic ovarian cyst. Sagittal T1 (**a**), T2 (**b**) and postcontrast T1 fat saturated (**c**) images show a T1 hypointense cyst with dependent hyperintensity (*arrowhead*) and predominant hyperintense signal with dependent hypointensity on T2 (*arrowhead*) and rim enhancement on postcontrast T1 image (*arrowhead*) suggestive of hemorrhagic cyst

Fig. 21 Infrarenal abdominal aortic aneurysm. Sagittal T1 (**a**) and axial T2 (**b**) images show aneurysmal dilatation of the infrarenal abdominal aorta (*arrows*), confirmed on postcontrast CT image (**c**) with eccentric atherosclerotic wall thickening on the right side (*arrowhead*)

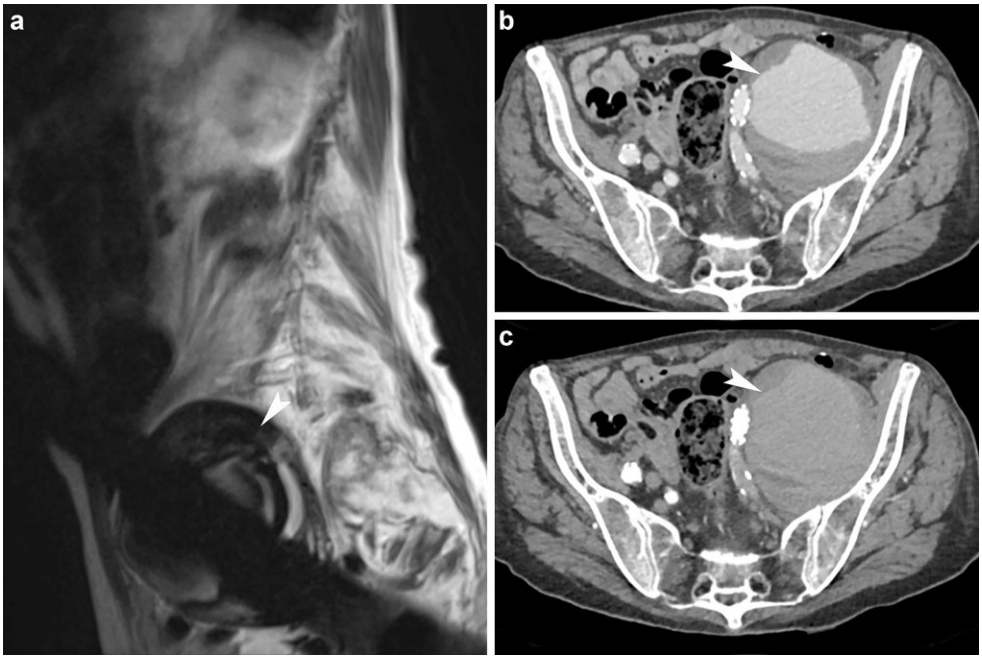

Fig. 22 Left iliac artery aneurysm. Sagittal T1 weighted image (**a**) shows a large oval lesion with signal void (*arrowhead*). Axial CT sections in early (**b**) and delayed (**c**) phases of contrast study show aneurysmal dilatation of the left external iliac artery with atherosclerotic wall thickening (*arrowhead*)

thickening in approximately 0.2% of individuals undergoing lumbar spine imaging [4–7]. Further evaluation and management of incidental uterine and bowel lesions depend on symptomatology and likelihood of underlying malignancy.

Well-defined ovarian cysts which show T2 hyperintense signal with a thin wall as well as the absence of internal septations, solid components, mural nodules and papillary projections are likely to be benign. Those that appear benign but cannot be completely evaluated, either due to artifacts or due to low signal to noise ratio, are defined as probably benign cysts. The presence of thick and nodular septations, solid component and papillary projections suggest a malignant etiology in cystic lesions. The recommendations for further evaluation of incidental ovarian cystic lesions depend on the age of the patient, and size and nature of the lesion. A simple cyst <3 cm is generally deemed a follicular cyst and needs no mention in the report or any further evaluation. Any benign appearing cyst >5 cm in a premenopausal woman and measuring 3–5 cm in an early postmenopausal woman (<5 years after menopause) needs follow-up ultrasound (US) after 6–12 weeks. A benign appearing lesion >5 cm in early postmenopausal and >3 cm in a late postmenopausal woman (>5 years after menopause) needs prompt US evaluation; however, the Society of Radiologists in Ultrasound (SRU) suggests further evaluation even for simple adnexal cysts >1 cm in postmenopausal women [87].

A hemorrhagic cyst usually shows T1 hyperintensity, shading sign on T2 weighted imaging and blooming on gradient echo due to blood products (Fig. 20). Any hemorrhagic lesion <5 cm in premenopausal women needs no further evaluation; however, larger lesions need prompt evaluation to rule out underlying malignancy [88]. A probable benign appearing lesion between 3–5 cm in a premenopausal woman needs follow-up ultrasound after 6–12 weeks. A probable benign appearing cyst >5 cm in premenopausal, >3 cm in early menopausal and >1 cm in late postmenopausal women needs prompt US evaluation. A lesion of any size with features suggestive of malignancy needs further evaluation [89].

Prostate enlargement can be seen in both benign and malignant conditions. Currently, unenhanced CT is limited to assess only the prostatic size. Postcontrast CT in the venous phase, whenever available needs to be evaluated for focal or mass-like enhancement. Although CT has a lower sensitivity, the presence of focal or mass-like enhancement has an agreement of 85% compared to multiparametric MRI in diagnosing prostate cancer [90]. Prostatic pathologies are categorized using the prostate imaging, reporting and data system (PI-RADS) after assessment of signal intensity on T2W imaging, presence or absence of restricted diffusion on diffusion-weighted imaging (DWI) and focal early enhancement on dynamic contrast-enhanced T1W imaging [91].

Vascular Lesions

Incidental vascular lesions include aortic and iliac artery aneurysms with aortic aneurysms seen in approximately 0.2% of individuals undergoing lumbar spine imaging [4–6]. The abdominal aorta is called ectatic when it measures >2.5 cm in diameter and an aneurysm is considered to exist when the diameter is >1.5 times normal size or >3 cm

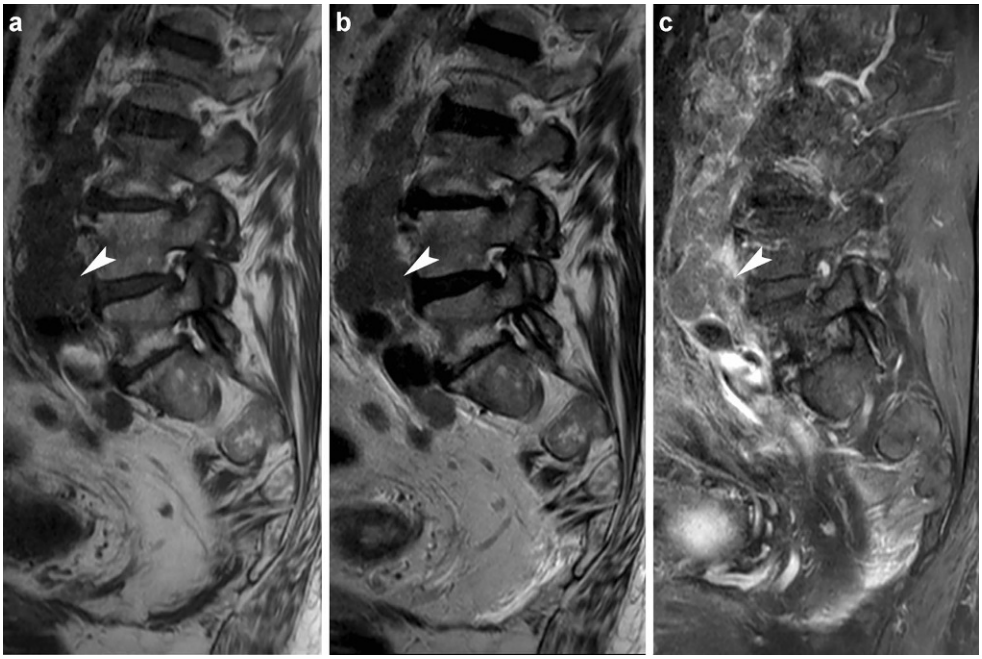

Fig. 23 Para-aortic lymphadenopathy. Sagittal T1 (**a**), T2 (**b**) and T1 fat saturated postcontrast (**c**) images show multiple enlarged lymph nodes (*arrowhead*) in the para-aortic region with isointense signal on T1 and T2 with no significant postcontrast enhancement

(Fig. 21). The recommendations for follow-up intervals and management of an aortic aneurysm depend predominantly on the risk factors, growth rate and diameter with frequent follow-up imaging recommended for aneurysms with larger diameter [92]. Iliac artery aneurysms are defined as a luminal diameter >1.5 times normal or >2.5 cm (Fig. 22). Iliac aneurysms between 3.0–3.5 cm are imaged after 6 months with follow-up imaging annually if they remain stable. Iliac aneurysms >3.5 cm need treatment or short interval follow-up imaging due to increased risk of rupture [92].

Miscellaneous Lesions

Lymphadenopathy is another common incidental finding on spine MRI. Further work-up of lymphadenopathy is based on the imaging findings, patient's clinical history, presence of risk factors to develop enlarged lymph nodes and comparison with previous imaging findings when available. The imaging findings to be assessed include size, site, number of nodes, nodal morphology, attenuation or signal intensity and enhancement characteristics. According to the response evaluation criteria in solid tumors (RECIST) working group, an enlarged node of >1 cm in short axis diameter is considered abnormal [93, 94]. Even though the significant size criteria remain unfounded, especially in retrocrural and periportal nodal stations, it may be appropriate to use the same criteria for all nodal stations. The presence of >3 nodes in a single nodal station or >2 nodes in >2 nodal stations is considered suspicious [95]. Normal lymph nodes are oval and elongated with a central fatty hilum. Enlarged nodes are usually round with increased short axis diameter and loss of fatty hilum, which may show increased enhancement in comparison to nodes in other stations, i. e., hypervascular nodes or heterogeneous enhancement with non-enhancing areas within suggesting necrosis. Patients with normal appearing lymph nodes and those with suspicious features which remain stable for 1 year are considered benign with no need for follow-up imaging or evaluation. In those with multiple enlarged nodes without apparent findings suggesting lymphoproliferative disorder, short-term follow-up after 3 months with CT or MRI is recommended. In patients with clinical, imaging or laboratory findings suggesting an underlying lymphoproliferative disorder; those with primary malignancy with propensity to metastasize and those with unstable disease on follow-up imaging need further evaluation with PET-CT or biopsy for further evaluation.

Enlarged nodes with preserved fatty halo and encapsulated mesenteric fat stranding, which are incidentally detected or may present with vague abdominal discomfort are suggestive of sclerosing mesenteritis [96]. The presence of lymphadenopathy in patients with an inflammatory process rules out other differential possibilities. Heterogeneous, enlarged pre-aortic and para-aortic lymph nodes can be due to underlying malignancy, inflammatory etiology and infectious causes, such as tuberculosis and rarely due to lymphoma (Fig. 23).

Conclusion

Incidental findings are common in spinal MRI. A systematic approach aids in assessment of these IFs particularly outside the clinical region of interest. When IFs are identi-

fied and their benign nature is uncertain, they can lead to increased patient anxiety and excessive medical expenditure; however, non-identification of malignant lesions can have devastating complications. Since radiologists are usually the first to detect these lesions, it is essential to be familiar with the recommendations of IFs, as the need for further evaluation and management when indicated must be mentioned in the report.

Conflict of Interest S.B. Hiremath, J. Boto, A. Regnaud, L. Etienne, A. Fitsiori and M.I. Vargas declare that they have no competing interests.

References

1. Incidental findings. American College of Radiology. 2018. https://www.acr.org/Clinical-Resources/Incidental-Findings. Accessed 19 Nov 2018.
2. Wagner SC, Morrison WB, Carrino JA, Schweitzer ME, Nothnagel H. Picture archiving and communication system: Effect on reporting of incidental findings. Radiology. 2002;225:500–5.
3. Ramadorai UE, Hire JM, DeVine JG. Magnetic resonance imaging of the cervical, thoracic, and lumbar spine in children: Spinal incidental findings in pediatric patients. Global Spine J. 2014;4:223–8.
4. Quattrocchi CC, Giona A, Di Martino AC, Errante Y, Scarciolla L, Mallio CA, Denaro V, Zobel BB. Extra-spinal incidental findings at lumbar spine MRI in the general population: A large cohort study. Insights Imaging. 2013;4:301–8.
5. Tuncel SA, Çaglı B, Tekataş A, Kırıcı MY, Ünlü E, Gençhellaç H. Extraspinal incidental findings on routine MRI of lumbar spine: Prevalence and reporting rates in 1278 patients. Korean J Radiol. 2015;16:866–73.
6. Dilli A, Ayaz UY, Turanlı S, Saltas H, Karabacak OR, Damar C, Hekimoglu B. Incidental extraspinal findings on magnetic resonance imaging of intervertebral discs. Arch Med Sci. 2014;10:757–63.
7. Kızılgöz V, Aydın H, Sivrioğlu AK, Özcan ÜC, Menderes U, Karayol SS, Erdem A. Incidences and reporting rates of incidental findings on lumbar, thoracic, and cervical spinal magnetic resonance images and extra-neuronal findings on brain magnetic resonance images. Eur Res J. 2018; https://doi.org/10.18621/eurj.379704.
8. Pooler BD, Kim DH, Lam VP, Burnside ES, Pickhardt PJ. CT Colonography reporting and data system (C-RADS): Benchmark values from a clinical screening program. AJR Am J Roentgenol. 2014;202:1232–7.
9. Milhorat TH. Classification of syringomyelia. Neurosurg Focus. 2000;8:E1.
10. Vandertop WP. Syringomyelia. Neuropediatrics. 2014;45:3–9.
11. Jones BV. Cord cystic cavities: Syringomyelia and prominent central canal. Semin Ultrasound Ct Mr. 2017;38:98–104.
12. Strahle J, Muraszko KM, Garton HJ, Smith BW, Starr J, Kapurch JR 2nd, Maher CO. Syrinx location and size according to etiology: Identification of Chiari-associated syrinx. J Neurosurg Pediatr. 2015;16:21–9.
13. Rodriguez A, Kuhn EN, Somasundaram A, Couture DE. Management of idiopathic pediatric syringohydromyelia. J Neurosurg Pediatr. 2015;16:452–7.
14. Timpone VM, Patel SH. MRI of a syrinx: Is contrast material always necessary? AJR Am J Roentgenol. 2015;204:1082–5.
15. Sen A. "Flow comp off": An easy technique to confirm CSF flow within syrinx and aqueduct. Indian J Radiol Imaging. 2013;23:97.
16. Roy AK, Slimack NP, Ganju A. Idiopathic syringomyelia: Retrospective case series, comprehensive review, and update on management. Neurosurg Focus. 2011;31:E15.
17. Nakamura M, Ishii K, Watanabe K, Tsuji T, Matsumoto M, Toyama Y, Chiba K. Clinical significance and prognosis of idiopathic syringomyelia. J Spinal Disord Tech. 2009;22:372–5.
18. Kernohan JW. The ventriculus terminalis: Its growth and development. J Comp Neurol. 1924;38:107–25.
19. Coleman LT, Zimmerman RA, Rorke LB. Ventriculus terminalis of the conus medullaris: MR findings in children. AJNR Am J Neuroradiol. 1995;16:1421–6.
20. Nassar SI, Correll JW, Housepian EM. Intramedullary cystic lesions of the conus medullaris. J Neurol Neurosurg Psychiatry. 1968;31:106–9.
21. Sigal R, Denys A, Halimi P, Shapeero L, Doyon D, Boudghène F. Ventriculus terminalis of the conus medullaris: MR imaging in four patients with congenital dilatation. AJNR Am J Neuroradiol. 1991;12:733–7.
22. Byrd SE, Harvey C, Darling CF. MR of terminal myelocystoceles. Eur J Radiol. 1995;20:215–20.
23. Erkan K, Unal F, Kiris T. Terminal syringomyelia in association with the tethered cord syndrome. Neurosurgery. 1999;45:1351–9. Discussion 1359–60.
24. Suh SH, Chung TS, Lee SK, Cho YE, Kim KS. Ventriculus terminalis in adults: Unusual magnetic resonance imaging features and review of the literature. Korean J Radiol. 2012;13:557–63.
25. de Moura Batista L, Acioly MA, Carvalho CH, Ebner FH, Tatagiba M. Cystic lesion of the ventriculus terminalis: Proposal for a new clinical classification. J Neurosurg Spine. 2008;8:163–8.
26. Ganau M, Talacchi A, Cecchi PC, Ghimenton C, Gerosa M, Faccioli F. Cystic dilation of the ventriculus terminalis. J Neurosurg Spine. 2012;17:86–92.
27. Finn MA, Walker ML. Spinal lipomas: Clinical spectrum, embryology, and treatment. Neurosurg Focus. 2007;23:E10.
28. Uchino A, Mori T, Ohno M. Thickened fatty filum terminale: MR imaging. Neuroradiology. 1991;33:331–3.
29. Brown E, Matthes JC, Bazan C, Jinkins JR. Prevalence of incidental intraspinal lipoma of the lumbosacral spine as determined by MRI. Spine. 1994;19:833–6.
30. Cools MJ, Al-Holou WN, Stetler WR Jr, Wilson TJ, Muraszko KM, Ibrahim M, La Marca F, Garton HJ, Maher CO. Filum terminale lipomas: Imaging prevalence, natural history, and conus position. J Neurosurg Pediatr. 2014;13:559–67.
31. Enzmann DR, Rubin JB, DeLaPaz R, Wright A. Cerebrospinal fluid pulsation: Benefits and pitfalls in MR imaging. Radiology. 1986;161:773–8.
32. Bradley WG, Kortman KE, Burgoyne B. Flowing cerebrospinal fluid in normal and hydrocephalic states: Appearance on MR images. Radiology. 1986;159:611–6.
33. Lisanti C, Carlin C, Banks KP, Wang D. Normal MRI appearance and motion-related phenomena of CSF. AJR Am J Roentgenol. 2007;188:716–25.
34. Dietemann JL, Bogorin A, Abu Eid M, Sanda R, Mourao Soares I, Draghici S, Rotaru N, Koob M. Tips and traps in neurological imaging: Imaging the perimedullary spaces. Diagn Interv Imaging. 2012;93:985–92.
35. Vargas MI, Delavelle J, Kohler R, Becker CD, Lovblad K. Brain and spine MRI artifacts at 3Tesla. J Neuroradiol. 2009;36:74–81.
36. Moes P, Maillot C. Superficial veins of the human spinal cord. An attempt at classification. Arch Anat Histol Embryol Norm Exp. 1981;64:5–110.
37. Lane JI, Koeller KK, Atkinson JL. Enhanced lumbar nerve roots in the spine without prior surgery: Radiculitis or radicular veins? AJNR Am J Neuroradiol. 1994;15:1317–25.
38. Tarlov IM. Spinal perineurial and meningeal cysts. J Neurol Neurosurg Psychiatry. 1970;33:833–43.

39. Nabors MW, Pait TG, Byrd EB, Karim NO, Davis DO, Kobrine AI, Rizzoli HV. Updated assessment and current classification of spinal meningeal cysts. J Neurosurg. 1988;68:366–77.
40. Guo D, Shu K, Chen R, Ke C, Zhu Y, Lei T. Microsurgical treatment of symptomatic sacral perineurial cysts. Neurosurgery. 2007;60:1059–65. Discussion 1065–6.
41. Lucantoni C, Than KD, Wang AC, Valdivia-Valdivia JM, Maher CO, La Marca F, Park P. Tarlov cysts: A controversial lesion of the sacral spine. Neurosurg Focus. 2011;31:E14.
42. Clarke G, Kapoor V, Baxter J. Are Tarlov cysts being identified and reported on lumbar spine MRI scan in patients with sciatica. Global Spine J. 2016;6(1_suppl) https://doi.org/10.1055/s-0036-1582706.
43. Murphy K, Oaklander AL, Elias G, Kathuria S, Long DM. Treatment of 213 patients with symptomatic Tarlov cysts by CT-guided Percutaneous injection of fibrin sealant. Ajnr Am J Neuroradiol. 2016;37:373–9.
44. Langdown AJ, Grundy JRB, Birch NC. The clinical relevance of Tarlov cysts. J Spinal Disord Tech. 2005;18:29–33.
45. Attiah MA, Syre PP, Pierce J, Belyaeva E, Welch WC. Giant cystic sacral schwannoma mimicking tarlov cyst: A case report. Eur Spine J. 2016;25:84–8.
46. Boukobza M, Roussel A, Fernandez-Rodriguez P, Laissy JP. Giant multiple and bilateral presacral Tarlov cysts mimicking adnexal mass—imaging features. Int Med Case Rep J. 2018;11:181–4.
47. Klimo P, Rao G, Brockmeyer D. Congenital anomalies of the cervical spine. Neurosurg Clin N Am. 2007;18:463–78.
48. Naguib M, Farag H, Abd El Wahab I. Anaesthetic considerations in Klippel-Feil syndrome. Can Anaesth Soc J. 1986;33:66–70.
49. Satpathy A, Sloan R, Bhoora IG. Compression fracture or butterfly vertebra: Diagnostic importance in a trauma setting. Ann R Coll Surg Engl. 2004;86:W41–W3.
50. Park JS, Eun JP, Lee HO. Anteroposterior spondyloschisis of atlas with bilateral cleft defect of posterior arch: A case report. Spine (Phila Pa 1976). 2011;36:E144-7.
51. Allam E, Zhou Y. Bipartite Atlas or jefferson fracture? A case series and literature review. Spine (Phila Pa 1976). 2015;40:E661-4.
52. Currarino G, Rollins N, Diehl JT. Congenital defects of the posterior arch of the atlas: A report of seven cases including an affected mother and son. AJNR Am J Neuroradiol. 1994;15:249–54.
53. Hyun G, Allam E, Sander P, Hasiak C, Zhou Y. The prevalence of congenital C1 arch anomalies. Eur Spine J. 2018;27:1266–71.
54. Kwon JK, Kim MS, Lee GJ. The incidence and clinical implications of congenital defects of Atlantal arch. J Korean Neurosurg Soc. 2009;46:522–7.
55. Elmalky MM, Elsayed S, Arealis G, Mehdian H. Congenital C1 arch deficiency: Grand Round presentation. Eur Spine J. 2013;22:1223–6.
56. O'Brien WT, Shen P, Lee P. The dens: Normal development, developmental variants and anomalies, and traumatic injuries. J Clin Imaging Sci. 2015;5:38.
57. Hughes RJ, Saifuddin A. Imaging of lumbosacral transitional vertebrae. Clin Radiol. 2004;59:984–91.
58. Rodallec MH, Feydy A, Larousserie F, Anract P, Campagna R, Babinet A, Zins M, Drapé JL. Diagnostic imaging of solitary tumors of the spine: What to do and say. Radiographics. 2008;28:1019–41.
59. Gaudino S, Martucci M, Colantonio R, Lozupone E, Visconti E, Leone A, Colosimo C. A systematic approach to vertebral hemangioma. Skeletal Radiol. 2015;44:25–36.
60. Morales KA, Arevalo-Perez J, Peck KK, Holodny AI, Lis E, Karimi S. Differentiating atypical Hemangiomas and metastatic vertebral lesions: The role of T1-weighted dynamic contrast-enhanced MRI. AJNR Am J Neuroradiol. 2018;39:968–73.
61. Shi YJ, Li XT, Zhang XY, Liu YL, Tang L, Sun YS. Differential diagnosis of hemangiomas from spinal osteolytic metastases using 3.0T MRI: Comparison of T1-weighted imaging, chemical-shift imaging, diffusion-weighted and contrast-enhanced imaging. Oncotarget. 2017;8:71095–104.
62. Dang L, Liu C, Yang SM, Jiang L, Liu ZJ, Liu XG, Yuan HS, Wei F, Yu M. Aggressive vertebral hemangioma of the thoracic spine without typical radiological appearance. Eur Spine J. 2012;21:1994–9.
63. Onitsuka H. Roentgenologic aspects of bone islands. Radiology. 1977;123:607–12.
64. Resnick D, Nemcek AA, Haghighi P. Spinal enostoses (bone islands). Radiology. 1983;147:373–6.
65. Greenspan A. Bone island (enostosis): Current concept—a review. Skeletal Radiol. 1995;24:111–5.
66. Ulano A, Bredella MA, Burke P, Chebib I, Simeone FJ, Huang AJ, Torriani M, Chang CY. Distinguishing untreated Osteoblastic metastases from Enostoses using CT attenuation measurements. AJR Am J Roentgenol. 2016;207:362–8.
67. Yamaguchi T, Suzuki S, Ishiiwa H, Ueda Y. Intraosseous benign notochordal cell tumours: Overlooked precursors of classic chordomas? Histopathology. 2004;44:597–602.
68. Yamaguchi T, Iwata J, Sugihara S, McCarthy EF Jr, Karita M, Murakami H, Kawahara N, Tsuchiya H, Tomita K. Distinguishing benign notochordal cell tumors from vertebral chordoma. Skeletal Radiol. 2008;37:291–9.
69. Nishiguchi T, Mochizuki K, Ohsawa M, Inoue T, Kageyama K, Suzuki A, Takami T, Miki Y. Differentiating benign notochordal cell tumors from Chordomas: Radiographic features on MRI, CT, and Tomography. AJR Am J Roentgenol. 2011;196:644–50.
70. Amer HZM, Hameed M. Intraosseous benign notochordal cell tumor. Arch Pathol Lab Med. 2010;134:283–8.
71. Lee SY, Landis MS, Ross IG, Goela A, Leung AE. Extraspinal findings at lumbar spine CT examinations: Prevalence and clinical importance. Radiology. 2012;263:502–9.
72. Miyakoshi A, Dalley RW, Anzai Y. Magnetic resonance imaging of thyroid cancer. Top Magn Reson Imaging. 2007;18:293–302.
73. Hoang JK, Langer JE, Middleton WD, Wu CC, Hammers LW, Cronan JJ, Tessler FN, Grant EG, Berland LL. Managing incidental thyroid nodules detected on imaging: White paper of the ACR incidental thyroid findings committee. J Am Coll Radiol. 2015;12:143–50.
74. Biederer J, Hintze C, Fabel M. MRI of pulmonary nodules: Technique and diagnostic value. Cancer Imaging. 2008;8:125–30.
75. Gravina M, Stoppino LP, Casavecchia G, Moffa AP, Vinci R, Brunetti ND, Di Biase M, Macarini L. Incidental Extracardiac findings and their characterization on cardiac MRI. Biomed Res Int. 2017;2017:2423546.
76. Cieszanowski A, Lisowska A, Dabrowska M, Korczynski P, Zukowska M, Grudzinski IP, Pacho R, Rowinski O, Krenke R. MR imaging of pulmonary nodules: Detection rate and accuracy of size estimation in comparison to computed Tomography. PLoS ONE. 2016;11:e0156272.
77. MacMahon H, Naidich DP, Goo JM, Lee KS, Leung ANC, Mayo JR, Mehta AC, Ohno Y, Powell CA, Prokop M, Rubin GD, Schaefer-Prokop CM, Travis WD, Van Schil PE, Bankier AA. Guidelines for management of incidental pulmonary nodules detected on CT images: From the Fleischner society 2017. Radiology. 2017;284:228–43.
78. Balogh J, Victor D 3rd, Asham EH, Burroughs SG, Boktour M, Saharia A, Li X, Ghobrial RM, Monsour HP Jr. Hepatocellular carcinoma: A review. J Hepatocell Carc. 2016;3:41–53.
79. Fateen W, Ryder SD. Screening for hepatocellular carcinoma: Patient selection and perspectives. J Hepatocell Carc. 2017;4:71–9.
80. Gore RM, Pickhardt PJ, Mortele KJ, Fishman EK, Horowitz JM, Fimmel CJ, Talamonti MS, Berland LL, Pandharipande PV. Management of incidental liver lesions on CT: A white paper of the ACR incidental findings committee. J Am Coll Radiol. 2017;14:1429–37.

81. Boland GW, Goldberg MA, Lee MJ, Mayo-Smith WW, Dixon J, McNicholas MM, Mueller PR. Indeterminate adrenal mass in patients with cancer: Evaluation at PET with 2-[F-18]-fluoro-2-deoxy-D-glucose. Radiology. 1995;194:131–4.
82. Mansmann G, Lau J, Balk E, Rothberg M, Miyachi Y, Bornstein SR. The clinically inapparent adrenal mass: Update in diagnosis and management. Endocr Rev. 2004;25:309–40.
83. Mayo-Smith WW, Song JH, Boland GL, Francis IR, Israel GM, Mazzaglia PJ, Berland LL, Pandharipande PV. Management of incidental adrenal masses: A white paper of the ACR incidental findings committee. J Am Coll Radiol. 2017;14:1038–44.
84. Wood CG 3rd, Stromberg LJ 3rd, Harmath CB, Horowitz JM, Feng C, Hammond NA, Casalino DD, Goodhartz LA, Miller FH, Nikolaidis P. CT and MR imaging for evaluation of cystic renal lesions and diseases. Radiographics. 2015;35:125–41.
85. Israel GM, Bosniak MA. Calcification in cystic renal masses: Is it important in diagnosis? Radiology. 2003;226:47–52.
86. Herts BR, Silverman SG, Hindman NM, Uzzo RG, Hartman RP, Israel GM, Baumgarten DA, Berland LL, Pandharipande PV. Management of the incidental renal mass on CT: A white paper of the ACR incidental findings committee. J Am Coll Radiol. 2018;15:264–73.
87. Levine D, Brown DL, Andreotti RF, Benacerraf B, Benson CB, Brewster WR, Coleman B, Depriest P, Doubilet PM, Goldstein SR, Hamper UM, Hecht JL, Horrow M, Hur HC, Marnach M, Patel MD, Platt LD, Puscheck E, Smith-Bindman R. Management of asymptomatic ovarian and other Adnexal cysts imaged at US: Society of radiologists in ultrasound consensus conference statement. Radiology. 2010;256:943–54.
88. Kobayashi H, Sumimoto K, Moniwa N, Imai M, Takakura K, Kuromaki T, Morioka E, Arisawa K, Terao T. Risk of developing ovarian cancer among women with ovarian endometrioma: A cohort study in Shizuoka, Japan. Int J Gynecol Cancer. 2007;17:37–43.
89. Patel MD, Ascher SM, Paspulati RM, Shanbhogue AK, Siegelman ES, Stein MW, Berland LL. Managing incidental findings on abdominal and pelvic CT and MRI, part 1: White paper of the ACR incidental findings committee II on adnexal findings. J Am Coll Radiol. 2013;10:675–81.
90. Jia JB, Houshyar R, Verma S, Uchio E, Lall C. Prostate cancer on computed tomography: A direct comparison with multi-parametric magnetic resonance imaging and tissue pathology. Eur J Radiol. 2016;85:261–7.
91. Weinreb JC, Barentsz JO, Choyke PL, Cornud F, Haider MA, Macura KJ, Margolis D, Schnall MD, Shtern F, Tempany CM, Thoeny HC, Verma S. PI-RADS prostate imaging—reporting and data system: 2015, version 2. Eur Urol. 2016;69:16–40.
92. Khosa F, Krinsky G, Macari M, Yucel EK, Berland LL. Managing incidental findings on abdominal and pelvic CT and MRI, part 2: White paper of the ACR incidental findings committee II on vascular findings. J Am Coll Radiol. 2013;10:789–94.
93. Eisenhauer EA, Therasse P, Bogaerts J, Schwartz LH, Sargent D, Ford R, Dancey J, Arbuck S, Gwyther S, Mooney M, Rubinstein L, Shankar L, Dodd L, Kaplan R, Lacombe D, Verweij J. New response evaluation criteria in solid tumours: Revised RECIST guideline (version 1.1). Eur J Cancer. 1990;45:228–47.
94. Schwartz LH, Litière S, de Vries E, Ford R, Gwyther S, Mandrekar S, Shankar L, Bogaerts J, Chen A, Dancey J, Hayes W, Hodi FS, Hoekstra OS, Huang EP, Lin N, Liu Y, Therasse P, Wolchok JD, Seymour L. RECIST 1.1—update and clarification: From the RECIST committee. Eur J Cancer. 2016;62:132–7.
95. Heller MT, Harisinghani M, Neitlich JD, Yeghiayan P, Berland LL. Managing incidental findings on abdominal and pelvic CT and MRI, part 3: White paper of the ACR incidental findings committee II on splenic and nodal findings. J Am Coll Radiol. 2013;10:833–9.
96. Sabaté JM, Torrubia S, Maideu J, Franquet T, Monill JM, Pérez C. Sclerosing mesenteritis: Imaging findings in 17 patients. AJR Am J Roentgenol. 1999;172:625–9.